

NEURAL FIELDS AND NOISE-INDUCED PATTERNS IN NEURONS ON LARGE DISORDERED NETWORKS

DANIELE AVITABILE* AND JAMES MACLAURIN †

Abstract. We study pattern formation in a class of high-dimensional neural networks posed on random graphs and subject to spatio-temporal stochastic forcing. Under generic conditions on coupling and nodal dynamics, we prove that the network admits a rigorous mean-field limit, resembling a Wilson-Cowan neural field equation. The state variables of the limiting systems are the mean and variance of neuronal activity. We select networks whose mean-field equations are tractable and we perform a bifurcation analysis using as control parameter the diffusivity strength of the afferent white noise on each neuron. We find conditions for Turing-like bifurcations in a system where the cortex is modelled as a ring, and we produce numerical evidence of noise-induced spiral waves in models with a two-dimensional cortex. We provide numerical evidence that solutions of the finite-size network converge weakly to solutions of the mean-field model. Finally, we prove a Large Deviation Principle, which provides a means of assessing the likelihood of deviations from the mean-field equations induced by finite-size effects.

1. Introduction. A key aspect of network dynamics, and in particular in mathematical neuroscience, is to understand how nodal (neuronal) dynamics, in combination with network (synaptic) structure, shapes patterns in spatially-extended networks. In deterministic systems with local interactions, a prominent mechanism for the onset of patterns from a homogeneous, quiescent state is the one proposed by Turing in the context of morphogenesis [74].

Turing's paradigm has been adopted and extended in numerous ways to explain pattern formation in natural systems (see [43, 44] for recent perspectives on Turing's work and influence). Turing bifurcations are typically studied in reaction-diffusion systems with local interactions, but instabilities with an identical bifurcation structure are also found in cortical models, in which neurons are coupled non-locally and without diffusion [37, 19, 27]. The mathematical treatment of these Turing-like bifurcations requires minor modifications, in order to deal with non-locality [36].

In the present paper we investigate the onset of patterns in randomly-connected neurons whose dynamics is also subject to noise. This research question is long standing: two early influential papers by Othmer and Scriven [64, 65] conjectured that large random networks could support pattern-forming instabilities in a mechanism analogous to the Turing instabilities for continuum PDEs. More recently, several groups worked theoretically, and experimentally on the impact of white noise on pattern formation [75, 79, 48, 38, 22, 57, 11], and it has been proposed that noise could explain why patterns are so prevalent in nature, despite the fact that often they can only be proven to exist in confined, and sometimes narrow, parametric regimes [56].

It has been conjectured that noise (both white noise temporal fluctuations, and disorder in the connectivity structure) is a key mechanism behind oscillations and rhythms in the brain [77, 48]. On the front of stochastic dynamics, early work by Scheutzow [67] demonstrated that mean-field systems can demonstrate oscillatory activity. More recently, Luçon and Poquet have demonstrated that white noise can

*Amsterdam Centre for Dynamics and Computation, Vrije Universiteit Amsterdam, Department of Mathematics, Faculteit der Exacte Wetenschappen, De Boelelaan 1081a, 1081 HV Amsterdam, The Netherlands. MathNeuro Team, Inria branch of the University of Montpellier, 860 rue Saint-Priest 34095 Montpellier Cedex 5 France. (d.avitabile@vu.nl, www.danieleavitabile.com, www.amsterdam-dynamics.nl).

†Department of Mathematical Sciences. New Jersey Institute of Technology,
james.n.maclaurin@njit.edu

excite oscillations in a high-dimensional all-to-all network of coupled excitable neurons [50, 52]. On the front of random connections, recent work by Bramburger and Holzer [15] tackled Turing bifurcations in the Swift-Hohenberg model on random graphs. Another recent work by Carrillo, Roux and Solem [22, 23] has proved the existence of noise-induced bifurcations in neural field equations.

In the present paper we study noise-induced bifurcations and noise-induced transitions in spatially-extended networks of n randomly-coupled, stochastically-forced neurons, which admit a tractable $n \rightarrow \infty$ limit, the so-called *mean-field limit*. The mean-field limit, in our case, pertains to the average and variance of the local neuronal activity, and resembles a *neural field equation*. Neural fields are heuristic models for the coarse-grained activity of spatially-extended neuronal network, which have been extensively employed by mathematical neuroscientists to predict a rich range of patterns, waves and other coherent structures [78, 3, 37, 19, 26, 27, 25].

An important open question concerns the derivation of neural-field equations as mean-field limits of microscopic neuronal models [18]. In this respect, the classical mean-field theory developed by McKean [58], Sznitman [69], and Tanaka [70] can be adapted to determine the large population-density limit of a network of neurons with a spatially-varying structure. Touboul [72, 71] has derived neural-field equations from particle models, with a connectivity that is a function of the spatial positions of the neurons. He found a range of interesting patterns and bifurcations, including standing waves and hopf bifurcations.

In this line of work [32, 49], neurons are thought of as interacting particles with heterogeneous coupling, and population-density evolution equations of McKean-Vlasov type are found in the mean-field limit. While such evolution equations can be derived in fairly general setups, their complexity often hinders further analysis, hence addressing questions concerning pattern formation, bifurcation, and noise-induced transitions remain often prohibitively difficult.

Further, the limiting equations are not necessarily similar to the classical Wilson-Cowan neural field equations [78], owing to differential operators featuring in the Fokker-Planck equation. From an intuitive standpoint, classical neural field equations are heuristic and reduce the neural activity at a spatial position to a finite set of variables; on the other hand, Fokker-Planck equations are rigorously derived, but contain the probabilistic distribution of all possible states at a particular spatial location. Our aim is to determine limiting equations that are as tractable as classical neural field equations, while being rigorously derived as the large n limit from a system of interacting neurons. One strategy to obtain limiting neural-field equations (both formally and rigorously) is to simplify the microscopic dynamics of neurons, so as to describe neuronal spikes as instantaneous events. Pattern formation in formal mean-field limits of integrate-and-fire spiking neurons have been recently studied, revealing that stationary patterns in the mean field may be a form of localised spatiotemporal chaos [7]. Further, neural-field equations have been found as rigorous limits of Hawkes Processes, in which the probability of a neuronal spike at a particular time is the average of the activity of other neurons. For this class of model, one can indeed achieve a limiting equation that resembles the classical Wilson-Cowan neural field equation, as long as the memory kernel is exponential [24, 2]. The state variable in the neural fields is the local spiking intensity function.

No large brain network is ‘all-to-all’. In fact typically most brain networks are sparse, insofar as the number of neurons connected to any particular neuron is much smaller than the total number of neurons in the network. We thus consider a general setup where the connectivity graph is inhomogeneous, and we make certain assump-

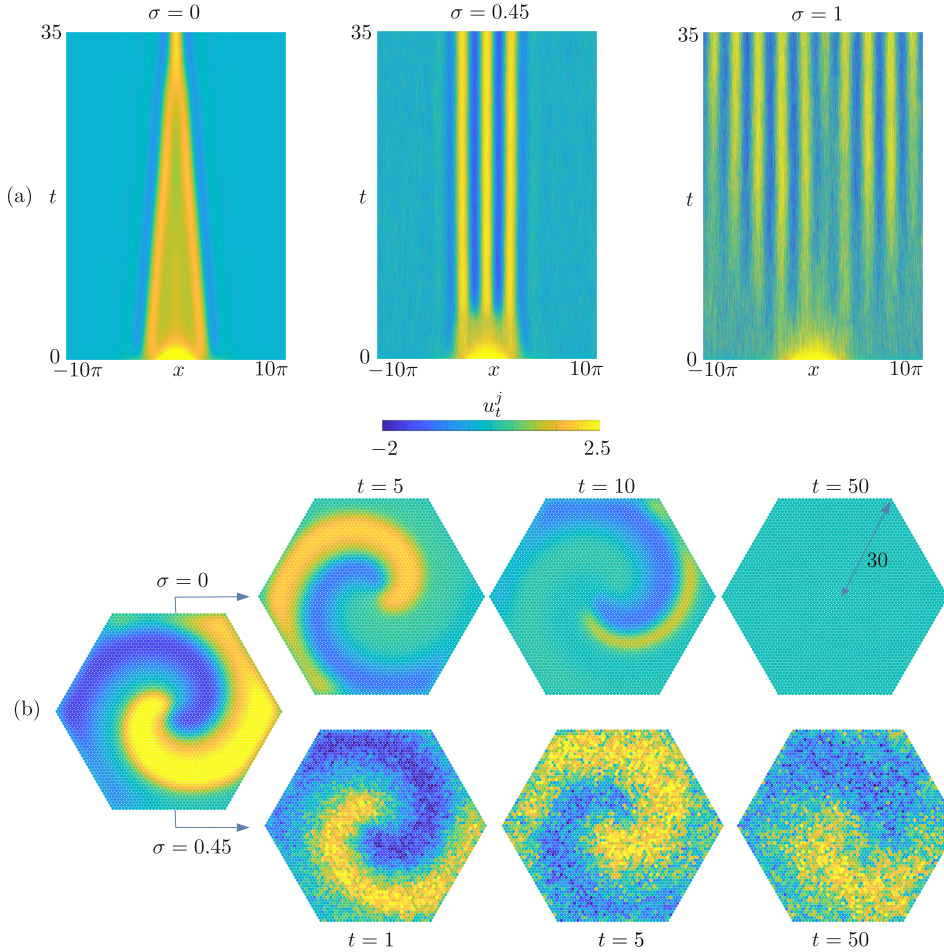


FIG. 1.1. Noise-induced spatiotemporal patterns. (a) A rate model with 2^{13} neurons, uniformly distributed on a ring of width 20π with all-to-all connections, displays a stationary localised equilibrium with 1 bump centred at $x = 0$ in the absence of noise; when parameters and initial conditions are fixed, and noise is switched on, the model displays a different localised solution, with 3 bumps at the core (noise intensity $\sigma = 0.45$), and a non-localised stationary state ($\sigma = 1$). (b) A rate model with 3367 sparsely-coupled neurons distributed on a hexagon with diameter 60 supports a persistent rotating wave when noise is present ($\sigma = 0.45$, [click here for an animation](#)), but the wave disappears when noise is absent ([click for animation](#)). Parameters: for (a) we have used the model detailed in subsection 5.4 with $L = 1$, $l = 10\pi$, $I(t, x) \equiv 0$, $G(x, t) \equiv \sigma$, $B = 0.4$, $\alpha = 10$, $\theta = 0.4$, $m_0(x) = 5/\cosh(0.25x)$; for (b) we use the model described in subsection 5.5 with $L_{11} = 1$, $L_{12} = 2$, $L_{21} = -0.44$, $L_{22} = 0.2$ $I(t, x) \equiv 0$, $G(x, t) \equiv \sigma$, $\nu = 1.5$, $\alpha = 10$, $\theta = 0.6$, with initial condition derived from a self-sustained spiral wave obtained in [6, Tutorial 2, and accompanying data].

tions on the average level of connectivity over the network. In the last section, we prove that these assumptions are satisfied if the connections were to be sampled independently from a distribution (with the probability of a connection depending on the spatial location of the two neurons). Indeed there has been considerable effort in recent years towards understanding dynamical systems on high dimensional random graphs [63, 31, 33, 12, 16, 76].

We work with McKean-Vlasov limits of spatially-extended neural networks of n

neurons of the form

$$(1.1) \quad du_t^j = \left(-Lu_t^j + \frac{1}{n\varphi_n} \sum_{k=1}^n K^{jk} f(u_t^k) + I_t^j \right) dt + G_t^j dW_t^j, \quad j = 1, \dots, n, \quad t \in \mathbb{R}_{\geq 0},$$

driven by independent \mathbb{R}^q -valued Brownian Motions $\{W_t^j\}_j$. Our choice for microscopic dynamics is thus a rate model: the variable u_t^j is a vector containing state variables of neuron at position x_n^j and time t ; in addition to membranal voltage, the vector may contain other neural variables such as synaptic or recovery variables; in addition, the form presented above is also a compact way of describing the dynamics of multiple co-located neuronal populations, whose variables at positions j are stacked into the vector u_t^j . Neurons are coupled through their firing rates f via the excitatory-inhibitory, and potentially sparse synaptic connections K^{jk} , with strengths that scale with n via the factor $n\varphi_n$, whose asymptotics as $n \rightarrow \infty$ will be discussed later. The network is subject to a deterministic external input, as well as additive noise, both of which have a spatio-temporal profile. In addition to stochastic forcing, the weights K are randomly distributed.

Crucially, we have kept the local neuronal dynamics linear, via the matrix L . Our mathematical derivation of the mean-field limit can be modified to account for nonlinear local interactions, but we refrain from this here: we rather leverage this choice to determine a limiting mean-field equation that resembles the Wilson-Cowan neural field equation.

In [Figure 1.1](#) we show two examples of noise-induced patterns in networks of type [\(1.1\)](#). In the first one neurons are distributed on a ring of width 20π and subject to a constant noise with intensity $G_t^j \equiv \sigma$. In the absence of noise, the network produces a localised stationary state with one bump at the core; upon increasing σ , while keeping all other elements of the model untouched, the system displays a localised state with 3 bumps at the core, or a nonlocalised state (see [Figure 1.1\(a\)](#)). The latter are not steady states in the particle system [\(1.1\)](#), because of the presence of stochastic forcing. Further, if we fix a spatial location j and time t , and send $n \rightarrow \infty$, the neuronal coordinates u_t^j in any ε -ball $B_\varepsilon(j)$ about x_n^j do not converge towards a limit: there is indeed no pointwise convergence of the spatial profiles, and indeed the higher n , the wider the fluctuations exhibited by the random variable u_t^j (that is, $\lim_{n \rightarrow \infty} \sup \{\|u_t^j\| : x_n^j \in B_\varepsilon(j)\} = \infty$).

The expectation and variance of u_t^j , however, converge to a limit as $n \rightarrow \infty$, and the evolution equation for their limits resemble Wilson-Cowan neural field equations, in which the noise intensity σ enters as a control parameter. The transitions seen in [Figure 1.1\(a\)](#) can thus be explained in the mean field limit by means of standard bifurcation theory, and numerical bifurcation analysis.

In [Figure 1.1\(b\)](#), we present an example in which neurons are distributed on a hexagon (note that the cortex here is a discrete lattice with around 3400 neurons, as visible from the image pixels and the [accompanying animations](#)). The vector u_t^j features a recovery variable, and the setup of this numerical experiment is inspired by a seminal paper by Huang et al. [40], in which spiral waves were observed in neocortical slices, and simulated with a neural field with a recovery variable. In [Figure 1.1\(b\)](#) we propose a simulation of a system of type [\(1.1\)](#): sufficiently large noise levels are necessary to support a rotating wave in the system, which decays towards the inactive state in the noiseless case.

The main results of the paper can be summarised as follows:

1. We provide conditions on [\(1.1\)](#) which guarantee that the empirical measure

associated to its particles converges as $n \rightarrow \infty$ to a unique measure. In addition to additive noise with spatio-temporal varying intensity, we work with quenched values of the random connections.

2. We prove that the marginal of the asymptotic measure is Gaussian at any spatial point, and any time. Further, we find that mean and variance of the law, which describe uniquely the marginal, evolve according to a system of neural-field equations.
3. Using a concrete example in which the mean field can be easily computed, we illustrate how noise-induced Turing-like bifurcations arise in the mean-field model: we use the noise intensity as the bifurcation parameter and show how a stable homogeneous state becomes unstable to periodic perturbations of predictable wavelength as the noise intensity increases.
4. We define an appropriate mode of convergence (weak convergence) for the random variables u_t^j to the mean-field variables, and provide numerical evidence that this mode of convergence is attained in numerical simulations.
5. We prove a Large Deviation Principle for the system.

The paper is structured as follows: we present notation in section 2, and introduce the particle model, our standing assumptions, and our main results in section 3; section 4 presents Turing-like bifurcations in a ring model, while section 5 discusses numerical experiments; we present mathematical proofs in section 6, and we conclude in section 7. Extra details for some of the proofs are provided in the supplementary materials.

2. Notation. For any Polish Space X , we let $\mathcal{P}(X)$ denote the set of all probability measures over X . We always endow $\mathcal{P}(X)$ with the topology of weak convergence: this is the unique topology such that $\mu_i \rightarrow \nu$ if and only if for any $g \in BC(X, \mathbb{R})$, the set of bounded continuous functions on X to \mathbb{R} , it holds $\mathbb{E}^{\mu_i}[g] \rightarrow \mathbb{E}^\nu[g]$, where for $\rho \in \mathcal{P}(X)$ we define

$$\mathbb{E}^\rho[g] = \int_X g(x) d\rho(x).$$

For $u \in C([0, T], \mathbb{R}^q)$, define the supremum norm

$$(2.1) \quad \|u\|_T = \sup_{t \in [0, T]} \sup_{1 \leq \alpha \leq q} |u_{\alpha, t}|.$$

More generally, for fixed compact $J \subset \mathbb{R}$ and Banach space X , we denote by $C(J, X)$ the space of continuous functions on J to X with norm

$$\|u\|_{C(J, X)} = \max_{t \in J} \|u(t)\|_X.$$

For an integer $n \in \mathbb{N}$ we set $\mathbb{N}_n = \{1, \dots, n\}$, and we denote by $\mathbb{R}^{n \times n}$ the space of real-valued n -by- n matrices, endowed with the Frobenius norm $\|\cdot\|_F$.

3. Particle Model. We introduce in this section a spatially-extended model of interacting neurons, subject to stochastic forcing, which we refer to as the *particle model*. The model features q populations of neurons, each containing n neurons, for a total of nq neurons. A straightforward adaptation of the model covers the case of population containing a variable number of neurons so that population α contains n_α neurons, for a total of $\sum_{\alpha=1}^q n_\alpha$ neurons. This choice would make notation heavier without modifying substantially our proofs, and we don't present it here. In passing we note that, without any modification, the q -population model presented below covers also the case of a single population of n neurons, each described by q variables.

The state of the system is described by a stochastic process $\{u_t : t \in [0, T]\}$ with values in \mathbb{R}^{nq} . It is convenient to expose the components of u_t , hence we set some notation to that purpose. Without loss of generality, we assume components to be ordered lexicographically and use the notation

$$u_{\alpha,t}^j := (u_t)_{(j-1)q+\alpha} \in \mathbb{R}, \quad (j, \alpha, t) \in \mathbb{N}_n \times \mathbb{N}_q \times [0, T]$$

to denote the state variable of neuron $j \in \mathbb{N}_n$ in population $\alpha \in \mathbb{N}_q$ (neuron (j, α)) at time $t \in \mathbb{R}_{\geq 0}$. Alternatively, in single population models in which each neuron configuration has multiple components, $u_{\alpha,t}^j$ represents the α th component of the state variable of neuron j at time t . With a little abuse of notation, we will use interchangeably $u_{\alpha,t}^j$ and $(u_t)_\alpha^j$. As we will see below, neurons are spatially distributed, with position x^j , and it is convenient to introduce a symbol for all state variables located at the j th node

$$u_t^j := \{u_{\alpha,t}^j\}_{j=1}^q \in \mathbb{R}^q \quad (j, t) \in \mathbb{R}^n \times [0, T].$$

The particle model is a system of nq Itô Stochastic Ordinary Differential Equations of the form

$$(3.1) \quad \begin{aligned} du_t^j &= \left(-Lu_t^j + \frac{1}{n\varphi_n} \sum_{k=1}^n K^{jk} f(u_t^j) + I_t^j \right) dt + G_t^j dW_t^j, \quad (j, t) \in \mathbb{N}_n \times [0, T], \\ u_0^j &= z^j, \quad j \in \mathbb{N}_n \end{aligned}$$

in which L and $\{K^{jk}\}_{j,k}$ are q -by- q matrices representing the local and nonlocal interaction coupling, respectively; φ_n is a coefficient scaling with n , the function $f: \mathbb{R}^q \rightarrow \mathbb{R}^q$ models neuronal firing rates, the vectors $\{I_t^j\}_j \subset \mathbb{R}^q$ model deterministic external inputs at time t , the q -by- q matrices $\{G_t^j\}_j$ model the intensity of the noise (the diffusion term) at time t , and $\{z^j\}_j \subset \mathbb{R}^q$ are the initial conditions. In the remainder of this section we shall present all elements of the model, so as to set the SODE on precise ground, and present our working assumptions.

3.1. Geometry. We begin by making assumptions on the geometry of the cortex. Neurons are spatially distributed on a cortex D for which we make the following standing assumption:

HYPOTHESIS 3.1 (Cortical domain). *The cortex D is a compact domain in \mathbb{R}^d , for $d \in \mathbb{N}$, and there exists a metric $d(\cdot, \cdot)$ which defines a topology on D .*

In applications, the choice $D = \mathbb{S}^1$ or $D = \mathbb{S}^2$ is sometimes convenient, but we are not restricted to this choice in the present paper. Further, neuron (j, α) occupies position $x_n^j \in D$ for any $\alpha \in \mathbb{N}_q$. In passing, note that we will omit the dependence on n for notational simplicity. Since x^j is independent of α , the q populations are co-located; this choice is also appropriate for a model with a single neuronal population of neurons described by q variables.

Neurons are distributed deterministically in D , but we are concerned with the limiting behaviour of the model when $n \rightarrow \infty$, for which we require the following assumption.

HYPOTHESIS 3.2 (Spatial distribution of neurons). *The empirical measure*

$$\hat{\mu}^n = \frac{1}{n} \sum_{j \in \mathbb{N}_n} \delta_{x_n^j} \in \mathcal{P}(D)$$

satisfies $\hat{\mu}^n \rightarrow \ell$ as $n \rightarrow \infty$ weakly in $\mathcal{P}(D)$, where ℓ is the uniform measure on D .

Remark 3.3. Although the distribution of points is deterministic, the empirical measure $\hat{\mu}^n(x)$ and its limit ℓ are still well-defined probability measures. This implies $\ell(D) = 1$ which differs from the Lebesgue measure of D as one may expect initially. An appropriate scaling that accounts for the Lebesgue measure of D will be introduced in due course.

3.2. Local and Nonlocal connectivity. The particle system (3.1) features both local and global neuronal interactions. The local interaction is given by the *deterministic, real-valued matrix* $L \in \mathbb{R}^{q \times q}$ hence a local (possibly self-) coupling is in place between neuron (j, α) and (j, β) . Note that, for simplicity, we have taken the matrix L to be spatially homogeneous, hence independent of j .

Remark 3.4. It is possible to derive mean-field limits for particle systems with nonlinear local dynamics [69]. In the present paper we aim to illustrate the phenomenon of noise-induced Turing-like patterns using a relatively simple setup, which favours mathematical tractability of the mean field over generality. In this spirit, we restrict our attention to linear local cross-population coupling between neuron (j, α) and (k, β) . We note that nonlinear effects are still present, through the mean-field coupling term discussed below.

The connection from neuron (k, β) to (j, α) is modelled via matrices $\{K^{jk}\}_{jk}$ acting on vectors $v \in \mathbb{R}^q$ as

$$(K^{jk}v)_\alpha = \sum_{\beta \in \mathbb{N}_q} K_{\alpha\beta}^{jk} v_\beta, \quad (j, k) \in \mathbb{N}_n.$$

The connectivity may be sparse or dense. The level of sparseness is indicated by a parameter φ_n : this is such that the typical number of edges afferent on a typical node is $n\varphi_n$. The synaptic connectivity can be excitatory and inhibitory, symmetric or asymmetric, and need not be distance dependent. We require the following hypothesis to hold, which is similar to a Graphon Assumption employed in many papers on high-dimensional deterministic ODEs on sparse networks [15].

HYPOTHESIS 3.5 (Synaptic connections). *The synaptic connection strength from neuron (k, β) to (j, α) is given by $(n\varphi_n)^{-1} K_{\alpha\beta}^{jk}$, with scaling factor $\varphi_n > 0$, and coefficient $K_{\alpha\beta}^{jk} \in \mathbb{R}$.*

1. *There exists a continuous function $\mathcal{K}_{\alpha\beta}: D \times D \rightarrow \mathbb{R}_{\geq 0}$ such that*

$$\lim_{n \rightarrow \infty} R^n = 0$$

where

$$R^n = n^{-1} \sup_{\alpha \in \mathbb{N}_q} \sup_{y \in [-1, 1]^{qn}} \sum_{j \in \mathbb{N}_n, \alpha \in \mathbb{N}_q} \left(n^{-1} \sum_{k \in \mathbb{N}_n, \beta \in \mathbb{N}_q} \left(\varphi_n^{-1} K_{\alpha\beta}^{jk} - \mathcal{K}_{\alpha\beta}(x_n^j, x_n^k) \right)^2 y_\beta^k \right).$$

2. *There exists a constant $c > 0$ such that $|K_{\alpha\beta}^{jk}| \leq c$ always.*
3. *The following limit is finite*

$$(3.2) \quad \overline{\lim}_{n \rightarrow \infty} (n\varphi_n)^{-1} \sup_{\alpha \in \mathbb{N}_q} \sup_{j \in \mathbb{N}_n} \sum_{k \in \mathbb{N}_n} \sum_{\beta \in \mathbb{N}_q} \chi\{K_{\alpha\beta}^{jk} \neq 0\} < \infty.$$

4. The limit $\lim_{n \rightarrow \infty} \varphi_n$ exists (and could be zero).

5. It holds that

$$\lim_{n \rightarrow \infty} n\varphi_n = \infty.$$

Intuitively, $\mathcal{K}_{\alpha\beta}(x, y)$ is a function representing the average connectivity from y to x , and [Theorem 3.5](#) is similar to an assumption on the convergence of a Graphon employed in many papers on high-dimensional deterministic ODEs on sparse networks [[15](#)]. There are several ways to employ these assumptions. One option is to simply take the connectivity to be such that $K_{\alpha\beta}^{jk} = \mathcal{K}_{\alpha\beta}(x_n^j, x_n^k)\varphi_n$, hence $\{K^{jk}\}_{jk} \subset \mathbb{R}^{q \times q}$ are deterministic matrices indicating connection strengths; in this case we say the particle model is *with kernel matrices*, as it uses directly the kernel functions $\mathcal{K}_{\alpha\beta}$.

Another option, which we refer to as *models with random ternary matrices*, is to use random ternary matrices $\{K^{jk}\}_{jk} \subset \{-1, 0, 1\}^{q \times q}$, whose values represent inhibitory, absent, and excitatory connections, respectively. In this case one assumes $K_{\alpha\beta}^{ab}$ is probabilistically dependent on $K_{\eta\zeta}^{ab}$ only if both $a = j$ and $b = k$; further, one chooses continuous functions $p_{\alpha\beta}^+, p_{\alpha\beta}^-: D \times D \rightarrow [0, 1] \subset \mathbb{R}$ such that $\mathcal{K}_{\alpha\beta}(x, y) = p_{\alpha\beta}^+(x, y) - p_{\alpha\beta}^-(x, y)$ and

$$(3.3) \quad \begin{aligned} \mathbb{P}(K_{\alpha\beta}^{jk} = -1) &= \varphi_n p_{\alpha\beta}^-(x_n^j, x_n^k), \\ \mathbb{P}(K_{\alpha\beta}^{jk} = 1) &= \varphi_n p_{\alpha\beta}^+(x_n^j, x_n^k), \\ \mathbb{P}(K_{\alpha\beta}^{jk} = 0) &= 1 - \varphi_n p_{\alpha\beta}^+(x_n^j, x_n^k) - \varphi_n p_{\alpha\beta}^-(x_n^j, x_n^k). \end{aligned}$$

In this case the kernel functions are linked to the probability measures for the connectivity (possibly via rescaling $\mathcal{K}_{\alpha\beta}$ by the constant c in [Theorem 3.5](#)). This method of constructing the random graph (by choosing the probability of a connection to be determined by the spatial positions of the nodes) is variously referred to as a stochastic block model, sparse Erdos-Renyi random graph, or W -random graph [[14](#)] in the literature.

Remark 3.6. In the Supplementary Material we prove that models with random ternary matrices satisfy [Theorem 3.5](#). Our numerical examples use by default models with kernel matrices, albeit [section 5](#) contains numerical results for both model types, and comparisons between each of them and the mean field.

3.3. Nonlinearities, external deterministic forcing, and diffusion term.

In order to complete the description of the particle system (3.1), we discuss the nonlinearities and forcing in the system.

Each neuron is described through a rate equation, with firing rate encoded in the nonlinearity $f: \mathbb{R}^q \times \mathbb{R}^q$, which is defined componentwise by

$$(f(v))_\alpha := f_\alpha(v_\alpha), \quad \alpha \in \mathbb{N}_q,$$

where $\{f_\alpha\}_\alpha$ are standard firing rate functions (more precise hypotheses will be given later).

The network is subject to an external deterministic forcing $I: [0, T] \times D \rightarrow \mathbb{R}^{nq}$, which appears in the particle model (3.1) via the position

$$(I_t^j)_\alpha := (I(t, x_n^j))_\alpha, \quad (j, \alpha, t) \in \mathbb{N}_n \times \mathbb{N}_q \times [0, T].$$

Similarly, the noise intensity is modelled via a deterministic mapping $G: [0, T] \times D \rightarrow \mathbb{R}^{q \times q}$, from which we extract matrices $\{G_t^j\}_{j,t} \subset \mathbb{R}^{q \times q}$ acting on vectors $v \in \mathbb{R}^q$

as

$$(G_t^j v)_\alpha = \sum_{\beta \in \mathbb{N}_q} (G(t, x_n^j))_{\alpha\beta} v_\beta, \quad (j, \alpha, t) \in \mathbb{N}_n \times \mathbb{N}_q \times [0, T].$$

3.4. Initial Conditions. The initial conditions are taken to be non-random constants. Throughout almost all of this paper it is assumed that the initial conditions $\{z^j\}_{j \in \mathbb{N}_n}$ are such that the following condition is satisfied.

HYPOTHESIS 3.7 (Initial Conditions). *There is a measure $\kappa \in \mathcal{P}(D \times \mathbb{R}^q)$ such that the empirical measure*

$$\hat{\mu}^n = \frac{1}{n} \sum_{j \in \mathbb{N}_n} \delta_{x_n^j, z^j} \in \mathcal{P}(D \times \mathbb{R}^q)$$

satisfies $\hat{\mu}^n \rightarrow \kappa \in \mathcal{P}(D \times \mathbb{R}^q)$ as $n \rightarrow \infty$. For $x \in D$, write $\kappa_x \in \mathcal{P}(\mathbb{R}^q)$ to be κ conditioned on its first variable x . It is assumed that κ_x is Gaussian, with mean $m_0(x) \in \mathbb{R}^q$ and covariance matrix $V_0(x) \in \mathbb{R}^{q \times q}$. Furthermore it is assumed that $x \mapsto m_0(x)$ and $x \mapsto V_0(x)$ are continuous.

In Corollary 3.12 we explain how this general assumption allows us to determine the limiting dynamics for a very broad class of initial conditions (in particular, if the initial conditions are sample from the large T equilibrium distribution).

Combining all terms we obtain a complete, component-wise version of the particle model (3.1),

$$(3.4) \quad \begin{aligned} du_{\alpha,t}^j &= \left[\sum_{\beta \in \mathbb{N}_q} \left(-L_{\alpha\beta} u_{\beta,t}^j + \frac{1}{n\varphi_n} \sum_{k \in \mathbb{N}_n} K_{\alpha\beta}^{jk} f_\beta(u_{\beta,t}^k) \right) + I_{\alpha,t}^j \right] dt \\ &\quad + \sum_{\beta \in \mathbb{N}_q} G_{\alpha\beta,t}^j dW_{\beta,t}^j, \quad (j, \alpha, t) \in \mathbb{N}_n \times \mathbb{N}_q \times \mathbb{R}_{\geq 0}, \\ u_{\alpha,0}^j &= z_\alpha^j, \quad (j, \alpha) \in \mathbb{N}_n \times \mathbb{N}_q \end{aligned}$$

We complete this section by making some assumptions on the functional inputs presented above

HYPOTHESIS 3.8 (Functional inputs to the particle system). *It holds that:*

1. *The average synaptic connectivity $K_{\alpha\beta}$ is in $C(D \times D, \mathbb{R})$ for all $\alpha, \beta \in \mathbb{R}^q$.*
2. *The firing rate function $f : \mathbb{R}^q \rightarrow \mathbb{R}^q$ is uniformly Lipschitz.*
3. *The firing rate function f is uniformly upperbounded.*
4. *The external input function I is in $C([0, T], C(D, \mathbb{R}^q))$.*
5. *The noise intensity function G is in $C([0, T], C(D, \mathbb{R}^{q \times q}))$.*
6. *The noise intensity also satisfies*

$$(3.5) \quad \inf_{t \in [0, T], x \in D} |\det(G(t, x))| > 0.$$

7. *The processes $\{W_t^j : t \in [0, T]\}_{j=1}^n$ are independent \mathbb{R}^q -valued Brownian Motions.*

Henceforth we will refer to Theorems 3.1 to 3.8 as our *standing assumptions* and we assume they hold throughout the rest of the paper.

Since the drift term in (3.4) is Lipschitz, it is well-known that there exists a unique strong solution [41]. By a ‘strong solution’, it is meant that for any valid probability space containing the Brownian Motions, initial conditions and random connections, there exists precisely one stochastic process u_t^j satisfying the above conditions.

3.5. Main results. We wish to study the empirical measure associated to a solution of the system in the interval $J = [0, T]$. For our treatment it is convenient to augment the orbit $\{u_t^j : t \in [0, T]\}$, so as to include also the positions $\{x^j\}_j$, which have trivial time-independent dynamics. We thus introduce the Banach space $(S_T, \|\cdot\|_{S_T})$ for this extended orbit of the system, by setting

$$S_T = D \times C([0, T], \mathbb{R}^q), \quad \| (x, u) \|_{S_T} = \| x \|_{\mathbb{R}^d} + \| u \|_T,$$

with $\|\cdot\|_T$ given in (2.1), and introduce the empirical measure

$$\hat{\mu}_T^n = \frac{1}{n} \sum_{j \in \mathbb{N}_n} \delta_{s^j} \quad s^j = (x^j, \{u_t^j : t \in [0, T]\}).$$

The empirical measure lives in the space

$$(3.6) \quad Y_T = \{ \mu \in \mathcal{P}(S_T) : \mathbb{E}^{s \sim \mu} [\|s\|_{S_T}] < \infty \},$$

and the topology of Y_T is metrized by the Wasserstein Distance, defined as follows

$$d_{Y_T}(\mu, \nu) = \inf_{\xi \in \Gamma(\mu, \nu)} \mathbb{E}^{(r, s) \sim \xi} [\|r - s\|_{S_T}],$$

where $\Gamma(\mu, \nu) \subset \mathcal{P}(S_T \times S_T)$ is the set of all couplings of μ and ν , that is, the subset of $\mathcal{P}(S_T \times S_T)$ so that the law of the random variable r under ξ is identical to μ , and the law of the random variable s under ξ is identical to ν .

Our first results concern the almost sure convergence of the empirical measure

THEOREM 3.9. *With probability one the empirical measure $\hat{\mu}_T^n$ converges as $n \rightarrow \infty$ to a unique measure $\mu_T \in Y_T$.*

We have specifically chosen a linear local interaction to ensure that μ_T admits a very tractable dynamics (i.e. one does not need to solve a PDE), and our next result concerns $\bar{\mu}_t \in \mathcal{P}(D \times \mathbb{R}^q)$, which we define to be the marginal of the limiting law at time t . This marginal is characterised in terms of a Gaussian distribution, whose mean and covariance satisfy a tractable integro-differential equation, resembling a neural field system.

LEMMA 3.10. *The marginal $\bar{\mu}_t$ can be written as the following probability law: for measurable subsets $A \subset D$, and $B \subseteq \mathbb{R}^q$,*

$$(3.7) \quad \bar{\mu}_t(A \times B) = \int_A \int_B \rho_q(m(t, x), V(t, x), u) du d\ell(x),$$

where ℓ is as in [Theorem 3.2](#), and where ρ_q , m , and V are defined below. The function $\rho_q: \mathbb{R}^q \times \mathbb{R}^{q \times q} \times \mathbb{R}^q \rightarrow \mathbb{R}_{>0}$ is the Gaussian density for a distribution with mean m and invertible covariance matrix V ,

$$\rho_q(m, V, u) = \frac{1}{\sqrt{(2\pi)^q \det(V)}} \exp\left(-\frac{1}{2}(u - m)^T V^{-1} (u - m)\right).$$

The mappings $m: [0, T] \times D \rightarrow \mathbb{R}^q$, and $V: [0, T] \times D \rightarrow \mathbb{R}^{q \times q}$ appearing in (3.7) are mean and covariance matrices of Gaussian variables, in the sense that for any $(t, x) \in [0, T] \times D$ there exists an \mathbb{R}^q -valued Gaussian variable $u_t(x)$ such that

$$\begin{aligned} m(t, x) &:= \mathbb{E}[u_t(x)] \\ V(t, x) &:= \mathbb{E}\left[\left(u_t(x) - m(t, x)\right)\left(u_t(x) - m(t, x)\right)^T\right]. \end{aligned}$$

Further, $t \mapsto (m(t, \cdot), V(t, \cdot))$ is the unique solution in $C^1([0, T], C(D, \mathbb{R}^q \times \mathbb{R}^{q \times q}))$ to the following initial-value problem

$$(3.8) \quad \begin{aligned} \partial_t m(t, x) &= -Lm(t, x) + \int_D \mathcal{K}(x, y) F(m(t, y), V(t, y)) \ell(dy) + I(t, x), \\ \partial_t V(t, x) &= -LV(t, x) - V(t, x)L^T + G(t, x)G^T(t, x), \\ m(0, x) &= m_0(x) \\ V(0, x) &= V_0(x) \end{aligned}$$

on $(t, x) \in [0, T] \times D$ in which $F: \mathbb{R}^q \times \mathbb{R}^{q \times q} \rightarrow \mathbb{R}^q$ given by

$$(3.9) \quad F(m, v) = \int_{\mathbb{R}^q} \rho_q(m, v, x) f(x) dx,$$

and with L , I , G , \mathcal{K} , f , m_0 , and V_0 given in Sections 3.2 and 3.3.

Remark 3.11. We remark that the mean field (3.8) is exact, in the sense that it does not involve an approximation or a truncation, and does not require expressions for the cross-variance at difference spatial positions to ‘close’ the dynamics. For a standard treatment of ODEs for the mean and variance of linear SDEs, we refer to [41, Section 5.6].

Most papers concerning the large size limiting behavior of neurons with sparse disordered connections assume that the initial conditions are sampled independently from the law of the random connections. A major strength of the results in this paper is that we do not require this assumption. See also a similar result due to Coppini [28]. We underscore this in the following corollary.

COROLLARY 3.12. Suppose that all of the previous assumptions hold, except that now the initial conditions $\{u_{\alpha,0}^j\}_{j \in \mathbb{N}_n, \alpha \in \mathbb{N}_q}$ are arbitrary constants. Let τ_n be any valid stopping time such that with unit probability,

$$(3.10) \quad \lim_{n \rightarrow \infty} n^{-1} \sum_{j \in \mathbb{N}_n} \delta_{x_n^j, u_{\tau_n}^j} = \kappa.$$

Then if we define $z^j := u_{\tau_n}^j$, the result in Theorem 3.9 holds (with the time defined relative to the stopping time, i.e. $t \rightarrow t - \tau_n$).

To see why this corollary must be true, one only needs to verify that Hypothesis 3.7 is indeed satisfied.

We refer the reader to [41] for a definition of stopping times. Essentially, it is any random time that ‘cannot know the future’: for example the following ‘first-hitting-time’ is a valid stopping time, for some $\zeta \in \mathcal{P}(D \times \mathbb{R}^q)$ and $\varepsilon_n > 0$,

$$\tau_n = \inf \left\{ t \geq 0 : d_W \left(n^{-1} \sum_{j \in \mathbb{N}_n} \delta_{x_n^j, u_t^j}, \zeta \right) \leq \varepsilon_n \right\}.$$

By contrast the following is not a valid stopping time, for any measurable $A \subseteq \mathbb{R}^{nq}$,

$$\tilde{\tau}_n = \inf \left\{ t \geq 0 : u_{t+1} \in A \right\}$$

3.6. Large Deviations Results. The importance of understanding how noise can induce rare events in biological systems is increasingly recognized [42, 20]. A key early study on this phenomenon was conducted by Newby, Keener and Bressloff

[62, 20, 61]. They determined that it is possible that small amounts of noise can induce rare events in excitable systems (such as spontaneous production of an action potential [42, 61]).

It is widely conjectured that noise-induced transitions between attractor states could be essential to the brain's proper functioning [30, 17]. Such transitions include UP / DOWN transitions [68], the wandering of bumps of activity in the visual cortex [55], and stochastic models of binocular rivalry [59]. For this reason, we also prove a Large Deviations Principle: this gives an asymptotic characterization of the probability of a transition path. It is significant to notice that the Large Deviations rate function is the same as the rate function with averaged connections (defined in the course of the proof). In other words, even for rare events, rare fluctuations in the sparse structure of the graph have a negligible effect.

THEOREM 3.13. *There exists a lower-semicontinuous function $\mathcal{J}_T : Y_T \rightarrow \mathbb{R}^+$ (specified further below in (6.9)) such that for any sets $\mathcal{A}, \mathcal{O} \subset Y_T$, with \mathcal{A} closed and \mathcal{O} open,*

$$(3.11) \quad \overline{\lim}_{n \rightarrow \infty} n^{-1} \log \mathbb{P}(\hat{\mu}_T^n \in \mathcal{A}) \leq - \inf_{\mu \in \mathcal{A}} \mathcal{J}_T(\mu)$$

$$(3.12) \quad \underline{\lim}_{n \rightarrow \infty} n^{-1} \log \mathbb{P}(\hat{\mu}_T^n \in \mathcal{O}) \geq - \inf_{\mu \in \mathcal{O}} \mathcal{J}_T(\mu).$$

Also \mathcal{J}_T has compact level sets.

4. Noise-induced Turing-like bifurcation. We illustrate the noise-induced mechanism for pattern-formation in its simplest form, by considering a one population network ($q = 1$) on a ring of width $2l$, $D = \mathbb{R}/2l\mathbb{Z}$ with distance dependent kernel $\mathcal{K}(x, y) = A(x - y)$, where $A \in C_p(2l, \mathbb{R})$, the space of continuous real-valued $2l$ -periodic functions. We consider a network with $L = 1$, $I(t, x) \equiv 0$, and time-independent, homogeneous noise intensity $G(t, x) \equiv \sigma$, for some $\delta \geq 0$. To illustrate the Turing bifurcation numerically we will select $l = 20\pi$, and we highlight that, upon rescaling space and parameters in the kernel A , the model can be equivalently posed on a ring of width π or 2π , thereby modelling orientation or direction preference, respectively [37, 27].

We show that a homogeneous steady state (m_*, v_*) of (3.8) which is linearly stable in the noiseless network ($\sigma = 0$) becomes linearly unstable to spatially-periodic perturbations for sufficiently large noise intensity σ .

Firstly, we note that the mean-field evolution for the covariance matrix V in (3.8) is decoupled from the mean evolution, and its dynamics is uniformly contracting over D , as the following lemma states.

LEMMA 4.1. *Suppose that $G_t(x)$ is independent of t and that there is a positive constant γ such that $\max\{\operatorname{Re} \lambda : \lambda \in \sigma(L)\} < -\gamma$, where $\sigma(L)$ is the spectrum of the matrix L . Then there exists a unique $V_*(x) \in C(D, \mathbb{R}^{Q \times Q})$ and constants $\beta, \varepsilon > 0$ such that for all $V_0 \in C(D, \mathbb{R}^{q \times q})$ and all $x \in D$,*

$$\|V(t, x) - V_*(x)\|_{C(D, \mathbb{R}^{q \times q})} \leq \beta e^{-\varepsilon t} \|V_0 - V_*(x)\|_{C(D, \mathbb{R}^{q \times q})}, \quad t \in \mathbb{R}_{\geq 0}.$$

Proof. See section A. □

For the network under consideration, homogeneous steady states are identified with $(m_*, v_*) \in \mathbb{R}^2$ satisfying the system

$$(4.1) \quad 0 = -m_* + F(m_*, \sigma^2/2) \int_{-l}^l A(x) dx, \quad v_* = \sigma^2/2,$$

from which we deduce that homogeneous steady states are parametrised by σ . Assuming a homogeneous steady state (m_*, v_*) exists, to assess linear its stability we must study the asymptotic behaviour of solutions to (3.8) of the form $(\tilde{m}(t, x), \tilde{v}(t, x)) = (m_* + m(t, x), v_* + v(t, x))$ for small (m, v) .

From Lemma 4.1, however, we know that $v(t, x) \equiv v_* = \sigma^2/2$ is a stable equilibrium of the covariance equation, which is decoupled from the dynamics of the mean m , hence perturbations to the initial conditions around v_* decay exponentially fast. Therefore we focus on the long-term behaviour of solutions to (3.8) of the form $(\tilde{m}(t, x), \tilde{v}(t, x)) = (m_* + m(t, x), v_*)$ for small m : in this setup the noise-induced Turing-like bifurcation is a Turing-like bifurcation of homogeneous steady states of (3.8), in the parameter σ for the problem

$$(4.2) \quad \partial_t m(t, x) = -m(t, x) + \int_{-l}^l A(x-y) F(m(t, y), \sigma^2/2) dy.$$

We will proceed formally. For a rigorous centre-manifold reduction of neural field equations around several instabilities, including a Turing-like bifurcation, we refer to [8]. We also refer to [22] for a rigorous treatment of Turing-like bifurcations in a nonlinear, nonlocal Fokker-Planck equation for neuronal dynamics.

Small perturbations $m(t, x)$ to m_* , under $v(x, t) \equiv \sigma^2/2$ are governed by the linearised evolution equation

$$(4.3) \quad \partial_t m(t, x) = -m(t, x) + D_m F(m_*, \sigma^2/2) \int_{-l}^l A(x-y) m(t, y) dy,$$

for $(t, x) \in \mathbb{R}_{\geq 0} \times \mathbb{R}/2l\mathbb{Z}$, in which we have denoted by $D_m F$ the derivative of F with respect to m , which is guaranteed to exist by (3.9). Linear stability is determined by long-term behaviour of solutions to the problem above, seen as an ODE on the Banach space $C_p(2l, \mathbb{C})$. Expressing the kernel $A \in C_p(2l, \mathbb{R})$ as a Fourier series

$$A(x) = \sum_{k \in \mathbb{Z}} A_k \varphi_k(x), \quad A_k = \frac{1}{2l} \int_{-l}^l A(x) \bar{\varphi}_k(x) dx, \quad \varphi_k(x) = e^{ik\pi x/l}, \quad k \in \mathbb{Z},$$

and using the periodic convolution theorem, we find that (4.3) admits solutions

$$m_k(t, x) = \exp(\lambda_k t + ik\pi x/l), \quad \lambda_k = -1 + D_m F(m_*, \sigma^2/2) 2l A_k \in \mathbb{C}, \quad k \in \mathbb{Z}.$$

A noise-induced Turing-like bifurcation occurs along on a branch of homogeneous steady states $\{m_*(\sigma) : \sigma \in I \subset \mathbb{R}\}$ if one of the eigenvalues of λ_k crosses the imaginary axis with nonzero speed, as σ varies. More precisely, the bifurcation occurs at $\sigma = \sigma_c$ if there exist $(\sigma_c, k_c) \in I \times \mathbb{Z}$ such that the mapping

$$(4.4) \quad \gamma_k : I \rightarrow \mathbb{R}, \quad \sigma \mapsto \operatorname{Re}[-1 + D_m F(m_*(\sigma), \sigma^2/2) 2l A_k]$$

satisfies the conditions $\gamma_{k_c}(\sigma_c) = 0$ and $\gamma'_{k_c}(\sigma_c) \neq 0$.

For suitable choices of kernel and firing rate function it is possible that a homogeneous equilibrium in the absence of noise, $m_*(0)$, is linearly stable while, upon increasing σ , the equilibrium $m_*(\sigma_c)$ becomes linearly unstable to perturbations with wavelength $k_c \pi/l$.

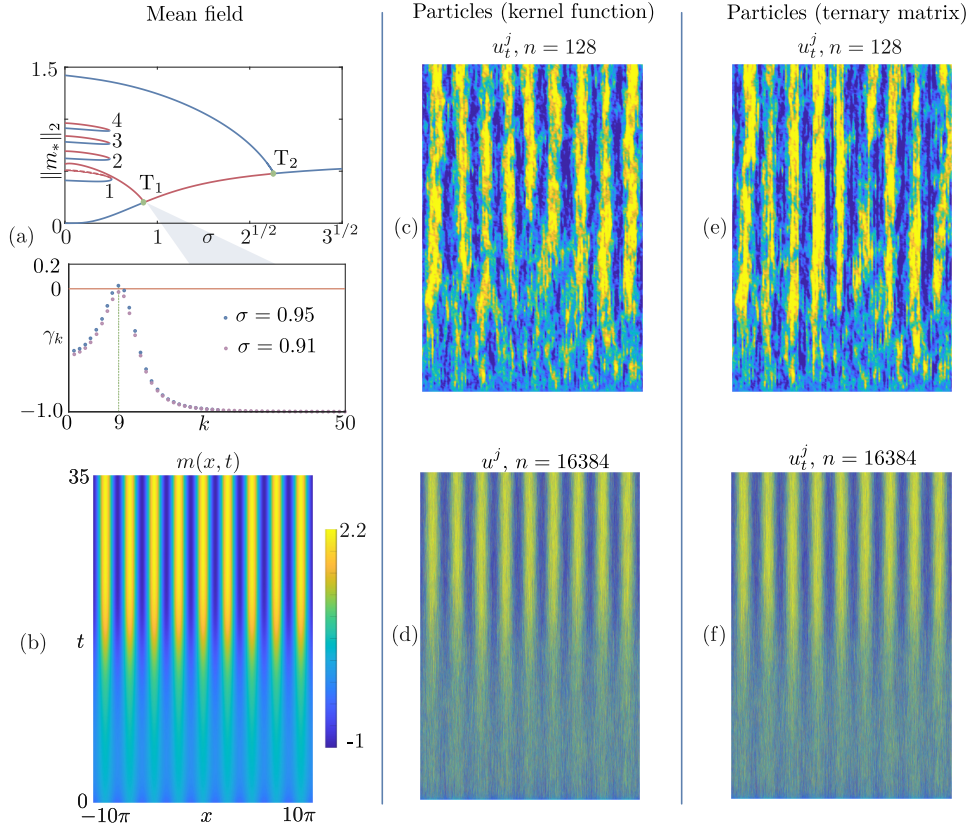


FIG. 5.1. Noise-induced Turing-like bifurcation for the particle and mean-field model with one population ($q = 1$), posed on a ring of width $2l$, with synaptic kernel (5.1), neuronal firing rate (5.2), and mean-field firing rate (5.3). (a) Bifurcation diagram of steady states $m_*(x)$ to the mean-field system in the parameter σ . The homogeneous steady state undergoes Turing-like bifurcations at T_1 and T_2 that generate one unstable (red) and one stable (blue) branch of spatially-periodic steady states, respectively. The mean field system also supports steady states that are spatially localised, with multiple bumps (branches with 1–4 bumps are reported here). In the inset, the values $\{\gamma_k\}_k$ (defined as in (4.4)) confirm that a Turing-like bifurcation of the homogeneous steady state is located between $\sigma = 0.95$ and $\sigma = 0.91$, with critical wavenumber $k_c = 9$. (b) Numerical simulation of the mean-field system for $\sigma = 1 > \sigma_c$ showing that the system reaches a stable, spatially-periodic steady state which, using the bifurcation diagram in (a), is deduced to be the one emanating from T_2 . (c,d) The simulation in (b) is repeated for the particle system (3.1) with kernel function for $n = 128$ and $n = 16384$, respectively. (e,f) As in (c,d) but for a particle model with one sample of ternary matrix specified using (3.3) and (5.4), $\varphi_n \equiv 1$, and driven by the same Brownian increments as in (c,d). Parameters: $L = 1$, $l = 10\pi$, $I(t, x) \equiv 0$, $G(x, t) \equiv \sigma$, $B = 0.4$, $C = 1$, $\alpha = 10$, $\theta = 0.9$, $m_0(x) = 0.3 \cos(k_c \pi x / l)$.

5. Numerical experiments. We now present numerical simulations on the particle and mean-field system, and we refer to [9] for a public repository with our codes. The particle system is simulated using a standard Euler-Maruyama scheme with timestep $dt = 0.01$. We discretise the mean field with the spectral collocation method proposed in [66] which is spectrally convergent [5], and use Matlab’s in-built ODE45 for time stepping. We employed numerical bifurcation analysis tools developed in [66, 4].

5.1. Example of noise-induced Turing-like bifurcation. To exemplify the phenomenon, we consider a network with $q = 1$ on a ring of width $2l$, $D = \mathbb{R}/2l\mathbb{Z}$ with distance dependent kernel $\mathcal{K}(x, y) = 2lA(x - y)$, where

$$(5.1) \quad A(x) = Ce^{-B|x|}(B \sin |x| + \cos x), \quad B, C \in \mathbb{R}_0$$

linear coupling $L = 1$, forcing $I(t, x) \equiv 0$, $G(t, x) \equiv \sigma$, and with firing rate function

$$(5.2) \quad f(u) = \Phi(\alpha(u - \theta)), \quad \Phi(u) = \frac{1}{2} \left[1 + \operatorname{erf} \left(\frac{u}{\sqrt{2}} \right) \right], \quad \alpha \in \mathbb{R}_{>0}, \quad \theta \in \mathbb{R},$$

which results in a mean-field firing rate of the form [73]

$$(5.3) \quad F(m, v) = \Phi \left(\alpha \frac{m - \theta}{\sqrt{1 + \alpha^2 v}} \right).$$

The kernel \mathcal{K} is known to support localised stationary solutions arranged in a snaking bifurcation structure for neural fields [46, 66], in additions to spatially-periodic solutions emerging from a Turing bifurcation.

We employed numerical bifurcation analysis tools to study the bifurcation structure of steady states to of the mean-field equation in the parameter σ (see Figure 5.1(a)). The primary bifurcation T_1 is subcritical, and a branch of unstable spatially-periodic steady states emerges from a branch of homogeneous steady states (bottom branch). In contrast, the secondary bifurcation, T_2 , is supercritical and gives rise to stable spatially-periodic equilibria. Further, the model supports localised solutions with 1–4 core bumps, which are not arranged in a snaking diagram here, but rather on disconnected branches. In the inset of Figure 5.1(a) we show $\{\gamma_k\}_{k \in \mathbb{N}_{50}}$ for two values of σ near T_1 , which provides evidence of a bifurcation at $\sigma_c \in (0.91, 0.95)$ with wavenumber $k_c = 9$.

5.2. Kernel and ternary-matrix models for varying number of particles. We carried out time simulations of the particle system with varying numbers of neurons, and of the mean-field equation to confirm the predictions of the numerical bifurcation analysis in Figure 5.1(c–f). Our first experiment, in Figure 5.1(c,d) confirms the predictions by keeping the same parameters as in Figure 5.1(b), but implements a particle model with various n , and kernel matrix induced by $\mathcal{K}(x, y) = 2lA(x - y)$ (see the end of subsection 3.2 to recall this setup), and $\varphi_n \equiv 1$.

Further, we repeat the experiment in Figure 5.1(c,d) by retaining parameters and Brownian increments, but for one sample of a model with ternary-based matrix. The kernel satisfies $|\mathcal{K}(x, y)| \leq 1$, hence we assign probabilities as in (3.3) with

$$(5.4) \quad p^+(x, y) = \max(\mathcal{K}(x, y), 0), \quad p^-(x, y) = \max(-\mathcal{K}(x, y), 0), \quad \varphi_n \equiv 1.$$

Further numerical evidence that the kernel- and ternary-matrix models agree with each other and with the mean-field model is given in Figure 5.2(b), in which we superimpose $m(x_j, T)$ (mean field) and u_T^j (particle models) for simulations leading to a localised and a spatially-periodic stable state. The kernel- and ternary-matrix models do not display appreciable differences hence, while the figures contain exactly three profiles at every point x_j , we display in the foreground the kernel-matrix model profile for $x \leq 0$, and the ternary-matrix one for $x > 0$, to highlight the similarity.

The latter numerical experiments bring naturally the question of how the particle system converges to the mean-field limit as the number n grows, and we now turn our attention to this.

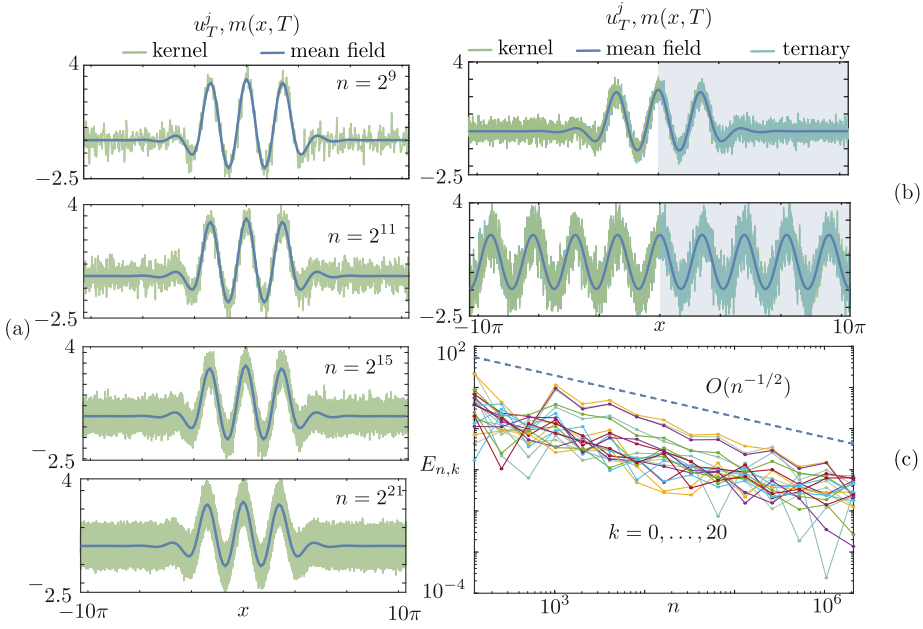


FIG. 5.2. *Convergence test for the particle and mean-field models with one population ($q = 1$), posed on a ring of width $2l$, with synaptic kernel (5.1), neuronal firing rate (5.2), and mean-field firing rate (5.3).* (a): Time simulations up to time $T = 35$ for increasing values of n approach a localised stationary state with 3 bumps in the core; we see that the profiles of the particle simulations (u_T^j , green) do not converge pointwise to the mean-field solution ($m(x, T)$, blue). (b) We superimpose the solution at $t = T$ of the mean field and both kernel- and ternary-matrix particle models with $n = 2^{12}$ for the simulation in (a), and for the one in Figure 5.1(c-f). The kernel- and ternary-matrix models do not display appreciable differences; note that the figures in (b) contain exactly three profiles at every point x_j , but we display in the foreground the kernel-matrix model profile for $x \leq 0$, and the ternary-matrix one for $x > 0$, to highlight the similarity. (c) The numerical simulations show that solutions to the particle system in (a) converge in weak sense to the mean-field state. The convergence is measured by $E_{n,k}$ as defined in (5.5), which occurs as an $O(n^{-1/2})$ for $k = 0, \dots, 20$. Parameters $L = 1$, $l = 10\pi$, $I(t, x) \equiv 0$, $G(x, t) \equiv \sigma$, $B = 0.4$, $C = 1$, $\alpha = 10$, $\theta = 0.9$; in (a), (b, top panel), and (c) $\sigma = 0.45$, and $m_0(x) = 5/\cosh(0.25x)$; in (b, bottom panel) $\sigma = 1$, $m_0(x) = 0.3 \cos(9\pi x/l)$; in the particle models we set $\varphi_n \equiv 1$.

5.3. Considerations on convergence. The empirical measure $\hat{\mu}_T^n$ is a mathematical object that facilitates an understanding of how the n -dimensional particle system can converge to a continuum limit [69]. Following from Theorem 3.9, we know that $\hat{\mu}_T^n$ converges to a unique measure μ_T weakly in Y_T , with probability one.

We are interested in characterizing the convergence of the marginals at particular times, hence we do not address, numerically, the convergence of the probability distribution across multiple times. We thus fix a particular time t for which we test convergence.

Let us suppose that $L^2(D)$ possesses a basis of orthonormal functions $\{\varphi_k\}_{k \in \mathbb{N}} \subset C(D)$. A natural choice would be the eigenvectors of the diffusion operator. Such a set is convergence-determining, meaning that two measures converge weakly if and only if their expectations of functions in this set converge. We thus test functions of the form $f_{k,\alpha}, g_{k,\alpha,\beta} : D \times \mathbb{R}^q \rightarrow \mathbb{R}$

$$f_{k,\alpha}(x, u) = \varphi_k(x)u_\alpha, \quad g_{k,\alpha,\beta}(x, u) = \varphi_k(x)u_\alpha u_\beta, \quad (k, \alpha) \in \mathbb{N} \times \mathbb{N}_q$$

for the mean and variance of $\hat{\mu}_t^n$, respectively. Note that technically, these functions

are not bounded (in contrast to what is required for two measures to converge weakly). However for our particular problem their expectations will also converge. This is proved in Corollary 0.5 in the Supplementary Materials.

One can thus study (numerically) the convergence of the following errors

$$E_{n,k}^m(t) = \max_{1 \leq \alpha \leq q} \left| \frac{1}{n} \sum_{j \in \mathbb{N}_n} \varphi_k(x_n^j) u_{\alpha,t}^j - \frac{1}{|D|} \int_D \varphi_k(x) m_\alpha(x, t) dx \right|,$$

$$E_{n,k}^V(t) = \max_{1 \leq \alpha, \beta \leq q} \left| \frac{1}{n} \sum_{j \in \mathbb{N}_n} \varphi_k(x_n^j) u_{\alpha,t}^j u_{\beta,t}^j - \frac{1}{|D|} \int_D \varphi_k(x) V_{\alpha\beta}(x, t) dx \right|,$$

for which we expect that asymptotics are of the form

$$E_{n,k}^m(t), E_{n,k}^V(t) \in O(n^{-1/2}), \quad \text{as } n \rightarrow \infty, \quad (k, t) \in \mathbb{N} \times [0, T]$$

This rate of convergence holds in the original work of Sznitman [69], and one also expects a Central Limit Theorem to hold (although this has not been proved in this paper). The disordered connections complicate an easy adaptation of the CLT in [69]. Coppini, Lucon and Poquet have proved a Central Limit Theorem for a similar disordered model [29].

5.4. Convergence. To test convergence in Figure 5.2 we have run a time simulation of the model with the new kernel up to $T = 35$, which was sufficient for the solution to approach a localised steady state with 3 bumps at the core. In addition to the mean-field simulation (in blue in Figure 5.2(a)), we have run simulations of the particle system (in green in Figure 5.2(a) for various number of n between 2^8 and 2^{21} . The data in Figure 5.2(a) shows that the particle system does not converge pointwise as $n \rightarrow \infty$, as we see an increasing variability in the spatial profiles u_T^j as $n \rightarrow \infty$. This is entirely what one would expect from our main result in Theorem 3.9, because the limiting Gaussian measure μ_T has nonzero variance.

The results in Theorem 3.9 (and following discussion) however, only concern the weak convergence of the empirical measure (see [13] for more explanation of this topology), hence we consider the following error

$$(5.5) \quad E_{n,k} = \left| \frac{2l}{n} \sum_{j=1}^n \varphi_k(x^j) u_T^j - \int_{-l}^l \varphi_k(x) m(x, T) dx \right|, \quad \varphi_k(x) = \exp(ik\pi x/l),$$

where $|\cdot|$ denotes the absolute value for complex numbers. In Figure 5.2(c) we plot $E_{n,k}$ as a function of n for $k = 0, \dots, 20$, and we find evidence that $E_{n,k} = O(n^{-1/2})$ for the tested values of k . This is precisely the rate of convergence that one expects from the Central Limit Theorem [39, 29] (although we have not proved a CLT in this paper).

5.5. Spiral wave simulations. Spiral waves experiments of Figure 1.1(b) have been carried out on a hexagonal cortex D inscribed in a disk of radius 30, in which neurons are uniformly distributed on a triangular grid (for details about meshing, and a similar spiral-wave simulation see [6, Tutorial 2]). See also recent work by Lucon and Poquet that identified oscillatory behavior in coupled Fitzhugh-Nagumo neurons [51].

The synaptic connection for the simulation are sparse, determined by a distance-dependent kernel $\mathcal{K}(r, r') = |D|\nu A(\|r - r'\|)$, where $|D|$ is the Lebesgue measure of

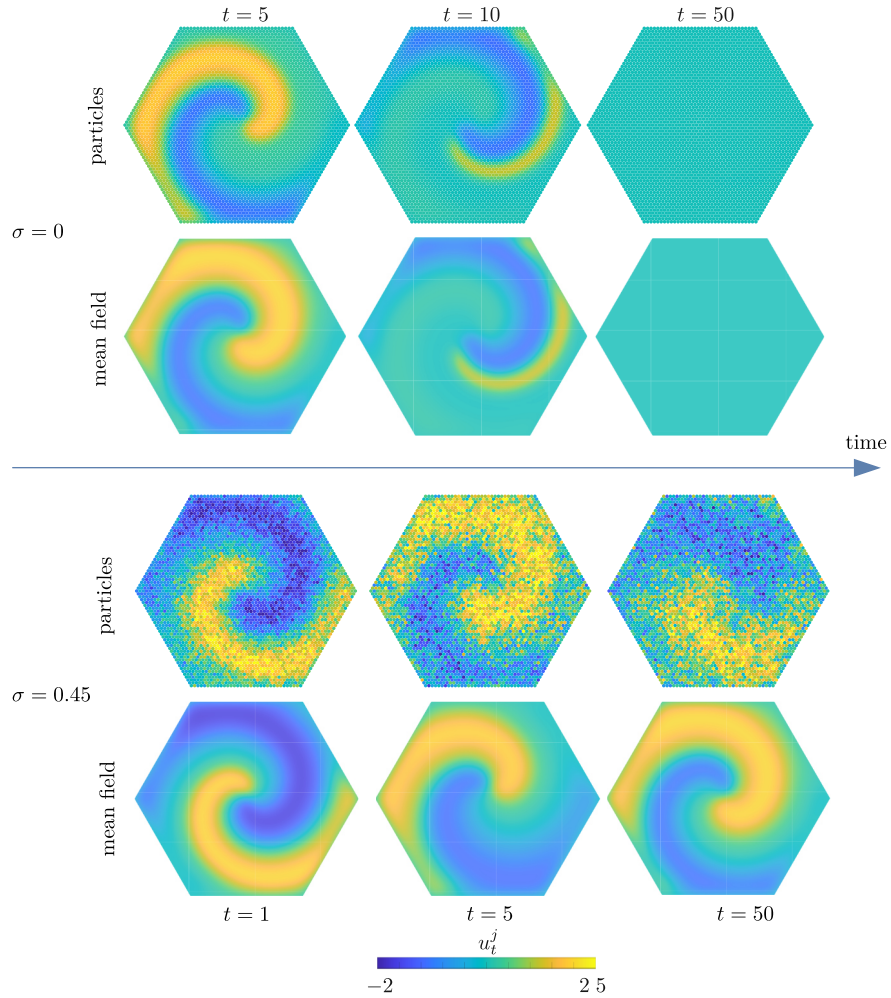


FIG. 5.3. Comparison between mean-field and particle model for the spiral wave simulations of Figure 1.1(b) for $\sigma = 0$ (top) and $\sigma = 0.45$ (bottom). In both cases a coherent structure is sustained only for sufficiently large values of σ . The wave in the particle simulation is influenced by noise, as expected. In the [accompanying animation](#), where the simulation is carried out for $t \in [0, 100]$ we see that the spiral wave in the particle model departs in phase from the one in the mean-field (see figure for $t = 50$) but regains phase on longer times. We highlight that, as discussed in subsection 5.4, we only expect weak (not pointwise) convergence. *In the particle model we set $\varphi_n \equiv 1$.*

D , with $\nu \in \mathbb{R}_{>0}$ and

$$A(x) = \begin{cases} a(x) & \text{if } |a(x)| > 10^{-3}, \\ 0 & \text{otherwise,} \end{cases} \quad a(x) = \int_0^\infty J_0(xs) \frac{s}{s^4 + s^2 + 1} ds.$$

The dynamics of the model includes a recovery variable therefore we have $q = 2$ in the particle system, and we set

$$L = \begin{bmatrix} L_{11} & L_{12} \\ L_{21} & L_{22} \end{bmatrix}, \quad f = \begin{bmatrix} \nu \Phi(\alpha(u - \theta)) \\ 0 \end{bmatrix},$$

with $\nu \in \mathbb{R}_{\geq 0}$ and Φ as in (5.2). In the simulation we also set $I(t, x) \equiv 0$ and

$G(t, x) \equiv \sigma$. It is possible to carry out a numerical bifurcation analysis for the spiral wave pattern in the parameter σ for the mean-field equations (see for instance [45]), along the lines of what was done for the ring model. We did not take this route here, and inspected the spiral wave onset with direct numerical simulation. The parameters in Figure 1.1(b) have been chosen so that the *mean-field model* with assigned initial condition $m(0, x)$ does not exhibit a stable spiral wave for $\sigma = 0$; in a set of simulations where $m(0, x)$ but σ was increased, we found values of σ for which a stable spiral wave is supported by the mean-field model. We then carried out numerical simulations for the particle model, to find an analogous behaviour. Figure 1.1 shows the spiral wave onset in the particle model, whereas Figure 5.3 compares simulations in the mean field and particle model. From the figure and the [accompanying animation](#) we see that the mean field and particle simulations produce both spiral waves, albeit the structure in the particle model displays transient phase slips, and it is visibly altered by noise. This is to be expected, in line of the weak convergence mode discussed in 5.3. Incidentally the transient phase slips are also entirely expected; this phenomenon is well-known in the Kuramoto model [10], see also [54, 1].

6. Proofs. The proofs employ the theory of Large Deviations [34], which characterizes the exponential asymptotics of the probability distribution for the system. The proofs proceed by comparing the disordered system to progressively simpler systems. In Section 6.1, we note the Large Deviations for the empirical measure generated by the Brownian Motions (this is a corollary of Sanov’s theorem). In Section 6.2, we prove a Large Deviation Principle for the system with averaged interactions by showing that its associated empirical measure can be written as a continuous mapping of the uncoupled empirical measure. This method of proof appears to have been pioneered by Tanaka [70], and more recently has been extended to spatially-distributed systems in [53]. Next, in Section 6.3, we prove a Large Deviation Principle for the system with disordered interactions by showing that the Radon-Nikodym derivative is relatively small, with extremely high probability. Finally, in Section 6.4, we prove that the Large Deviations rate function has a unique zero, and this yields the limiting equations. Extra details are provided in the Supplementary Materials.

6.1. Large Deviations of the Uncoupled System. In this section we outline the Large Deviations of the empirical measure generated by independent Brownian Motions. This theory is already known and is essentially due to Sanov [34]. The result in this section is useful because in the following section we demonstrate that the empirical measure for the coupled system can be obtained by applying a continuous transformation to the empirical measure resulting from the Brownian Motions.

We define the \mathbb{R}^q -valued random variables \tilde{W}_t^j with components given by

$$\tilde{W}_{\alpha,t}^j := (\tilde{W}_t^j)_\alpha = \int_0^t \sum_{\beta=1}^q G_{\alpha\beta}(s, x_n^j) dW_{\beta,s}^j.$$

We introduce the Banach space $(B_T, \|\cdot\|_{B_T})$ with

$$B_T = D \times \mathbb{R}^q \times C([0, T], \mathbb{R}^q), \quad \|(x, z, w)\|_{B_T} = \|x\|_{\mathbb{R}^d} + \|z\|_{\mathbb{R}^q} + \|w\|_T,$$

and study the convergence of the following empirical measure up to time T

$$(6.1) \quad \tilde{\mu}_T^n = n^{-1} \sum_{j \in \mathbb{N}_n} \delta_{b^j} \quad b^j = (x^j, u_0^j, \{\tilde{W}_t^j : t \in [0, T]\}),$$

which lives in the space

$$(6.2) \quad X_T = \{\mu \in \mathcal{P}(B_T) : \mathbb{E}^{b \sim \mu} [\|b\|_{B_T}] < \infty\}.$$

The topology of X_T is metrized by the Wasserstein Distance, defined as follows. For $\mu, \nu \in X_T$, we define

$$d_{X,T}(\mu, \nu) = \inf_{\xi \in \Gamma(\mu, \nu)} \mathbb{E}^{(b, \tilde{b}) \sim \xi} [\|b - \tilde{b}\|_{B_T}],$$

where as previously $\Gamma(\mu, \nu)$ is the set of all couplings between μ and ν .

Next we define the rate function $\mathcal{I}_T(\mu)$ that governs the Large Deviations of $\tilde{\mu}_T^n$. To this end, for $x \in D$, let $\mathcal{W}_T(x) \in \mathcal{P}(\mathbb{R}^q \times C([0, T], \mathbb{R}^q))$ be the law of Gaussian processes $\{w_{\alpha,t}(x) : \alpha \in \mathbb{N}_q, t \in [0, T]\}$ with the following covariance structure:

1. For any $(\alpha, t) \in \mathbb{N}_q \times [0, T]$, $w_{\alpha,t}(x)$ has zero mean;
2. For any $\alpha, \beta \in \mathbb{N}_q$ it holds

$$\mathbb{E}[w_{\alpha,s}(x)w_{\beta,t}(x)] = \int_0^s \sum_{\gamma=1}^q G_{\alpha\gamma,r}(x)G_{\beta\gamma,r}(x)dr, \quad s \leq t \leq T.$$

We first stipulate that $\mathcal{I}_T(\mu) := \infty$ if the marginal of μ over its first two variables is not equal to κ (recall that κ is the measure over $D \times \mathbb{R}^q$ that the empirical measure at time 0 converges to). Otherwise for $\mu \in X_T$, $x \in D$ and $z \in \mathbb{R}^q$ let $\mu_{x,z} \in \mathcal{P}(C([0, T], \mathbb{R}^q))$ denote the law of μ conditioned on the values of its first two variables. We can now define

$$(6.3) \quad \mathcal{I}_T(\mu) := \int_{D \times \mathbb{R}^q} \mathcal{R}(\mu_{x,z} || \mathcal{W}_T(x)) \kappa(dx, dz),$$

where $\mathcal{R}(\cdot || \cdot)$ is the Relative Entropy [21]. Note that we are following the ‘ $0 \times \infty = 0$ ’ convention in (6.3).

The following result is a well-known corollary of Sanov’s Theorem [34].

THEOREM 6.1. *Let $\mathcal{A}, \mathcal{O} \subseteq X_T$ be (respectively) closed and open. Then*

$$(6.4) \quad \overline{\lim}_{n \rightarrow \infty} n^{-1} \log \mathbb{P}(\tilde{\mu}_T^n \in \mathcal{A}) \leq - \inf_{\mu \in \mathcal{A}} \mathcal{I}_T(\mu)$$

$$(6.5) \quad \underline{\lim}_{n \rightarrow \infty} n^{-1} \log \mathbb{P}(\tilde{\mu}_T^n \in \mathcal{O}) \geq - \inf_{\mu \in \mathcal{O}} \mathcal{I}_T(\mu).$$

Furthermore $\mu \mapsto \mathcal{I}_T(\mu)$ is lower semi-continuous, and has compact level sets.

6.2. Large Deviations of the Averaged System. The main result of this section is that the system with averaged non-random connectivity is a tight approximation to the system with random connectivity, on an exponential scale. The proof proceeds by pushing-forward the empirical measure generated by the Brownian Motions by a continuous mapping. This technique was employed in the seminal work of Tanaka [70], and more recently has been employed for a spatially-distributed system in [53]. We introduce the n -dimensional system with averaged connectivity,

$$(6.6) \quad \begin{aligned} dv_{\alpha,t}^j &= \left(- \sum_{\beta=1}^q L_{\alpha\beta} v_{\beta,t}^j + n^{-1} \sum_{k=1}^n \sum_{\beta=1}^q \mathcal{K}_{\alpha\beta}(x_n^j, x_n^k) f_\beta(v_t^k) + I_{\alpha,t}(x_n^j) \right) dt \\ &\quad + \sum_{\beta=1}^q G_{\alpha\beta,t}(x_n^j) dW_{\beta,t}^j, \end{aligned}$$

$$v_\alpha^i = z_\alpha^i$$

which shares with the particle system (3.4) identical Brownian motions and initial conditions. We then define the empirical measure for the system with averaged interactions

$$(6.7) \quad \hat{\mu}_T^n = n^{-1} \sum_{j=1}^n \delta_{x_n^j, v^j} \in Y_T.$$

with Y_T given by (3.6). In the Supplementary Materials, we prove the following lemma.

LEMMA 6.2. *There exists a continuous function $\Phi_T : X_T \mapsto Y_T$ such that, with unit probability,*

$$(6.8) \quad \hat{\mu}_T^n = \Phi_T(\tilde{\mu}_T^n).$$

Next, define the rate function $\mathcal{J}_T : Y_T \rightarrow \mathbb{R}$ to be such that

$$(6.9) \quad \mathcal{J}_T(\mu) := \inf \{ \mathcal{I}_T(\nu) : \mu = \Phi_T(\nu) \}.$$

This leads us to a Large Deviation Principle for the averaged system.

LEMMA 6.3. *For any sets $\mathcal{A}, \mathcal{O} \subset Y_T$, with \mathcal{A} closed and \mathcal{O} open,*

$$(6.10) \quad \overline{\lim}_{n \rightarrow \infty} n^{-1} \log \mathbb{P}(\hat{\mu}_T^n \in \mathcal{A}) \leq - \inf_{\mu \in \mathcal{A}} \mathcal{J}_T(\mu)$$

$$(6.11) \quad \underline{\lim}_{n \rightarrow \infty} n^{-1} \log \mathbb{P}(\hat{\mu}_T^n \in \mathcal{O}) \geq - \inf_{\mu \in \mathcal{O}} \mathcal{J}_T(\mu).$$

Furthermore $\mu \mapsto \mathcal{J}_T$ is lower semi-continuous, and \mathcal{J}_T has compact level sets.

Proof. Since

$$(6.12) \quad \hat{\mu}_T^n = \Phi_T(\tilde{\mu}_T^n),$$

and Φ_T is continuous, the Large Deviation Principle must hold with rate function \mathcal{J}_T , thanks to the Contraction Principle [34]. \square

6.3. Disordered Coupling. In this section, we use the Large Deviations result of the system with averaged interactions (as proved in Lemma 6.3) to characterize the Large Deviations of the system with disordered interactions. We start by restating Theorem 3.13.

THEOREM 6.4. *For any sets $\mathcal{A}, \mathcal{O} \subset Y_T$, such that \mathcal{A} is closed and \mathcal{O} is open,*

$$(6.13) \quad \overline{\lim}_{n \rightarrow \infty} n^{-1} \log \mathbb{P}(\hat{\mu}_T^n \in \mathcal{A}) \leq - \inf_{\mu \in \mathcal{A}} \mathcal{J}_T(\mu)$$

$$(6.14) \quad \underline{\lim}_{n \rightarrow \infty} n^{-1} \log \mathbb{P}(\hat{\mu}_T^n \in \mathcal{O}) \geq - \inf_{\mu \in \mathcal{O}} \mathcal{J}_T(\mu).$$

Let $P^n \in \mathcal{P}(\mathcal{C}([0, T], \mathbb{R}^{qn}))$ be the law of the stochastic processes $(v_t^j)_{j \in \mathbb{N}_n, t \in [0, T]}$ and let $Q^n \in \mathcal{P}(\mathcal{C}([0, T], \mathbb{R}^{qn}))$ be the law of the original particle system $(u_t^j)_{j \in \mathbb{N}_n, t \in [0, T]}$. Write

$$(6.15) \quad z_{\alpha, t}^j = n^{-1} \sum_{\beta \in \mathbb{N}_q} \sum_{k \in \mathbb{N}_n} (\varphi_n^{-1} K_{\alpha\beta}^{jk} - \mathcal{K}_{\alpha\beta}(x_n^j, x_n^k)) f_\beta(u_t^k).$$

Thanks to Girsanov's Theorem [47]

$$(6.16) \quad \frac{dQ^n}{dP^n} = \exp(n\Gamma_n(u)),$$

where $\Gamma_n : \mathcal{C}([0, T], \mathbb{R}^{qn}) \rightarrow \mathbb{R}$ is such that, writing $H(t, x) := (H_{\alpha\beta}(t, x))_{\alpha, \beta \in \mathbb{N}_n} \in \mathbb{R}^{q \times q}$ to be the matrix inverse of $G(t, x)G(t, x)^T$,

$$(6.17) \quad \Gamma_n(u) = n^{-1} \sum_{j \in \mathbb{N}_n} \sum_{\alpha, \beta \in \mathbb{N}_q} \int_0^T \left\{ z_{\beta, s}^j H_{\alpha\beta}(s, x_n^j) \left(du_{\alpha, s}^j - \sum_{\gamma \in \mathbb{N}_q} L_{\alpha\gamma} u_{\gamma, s}^j ds \right. \right. \\ \left. \left. - n^{-1} \varphi_n^{-1} \sum_{k \in \mathbb{N}_n} \sum_{\gamma \in \mathbb{N}_q} K_{\alpha\gamma}^{jk} f(u_{\gamma, s}^k) ds \right) - \frac{1}{2} z_{\beta, s}^j z_{\alpha, s}^j H_{\alpha\beta}(s, x_n^j) \right\} ds.$$

We first show that Γ_n is small with very high probability.

LEMMA 6.5. *For any $\varepsilon > 0$,*

$$(6.18) \quad \overline{\lim}_{n \rightarrow \infty} n^{-1} \log \mathbb{P}(|\Gamma_n(u)| \geq \varepsilon) = -\infty.$$

Proof. It suffices to prove that for any $\ell, \varepsilon > 0$,

$$(6.19) \quad \overline{\lim}_{n \rightarrow \infty} n^{-1} \log \mathbb{P}(|\Gamma_n(u)| \geq \varepsilon) \leq -\ell.$$

Through rearranging, we find that Q^n -almost-surely,

$$(6.20) \quad \Gamma_n(u) = \frac{1}{2n} \sum_{j \in \mathbb{N}_n} \sum_{\alpha, \beta \in \mathbb{N}_q} \int_0^T z_{\beta, s}^j z_{\alpha, s}^j H_{\alpha\beta}(s, x_n^j) ds + X_T,$$

where

$$X_t = n^{-1} \sum_{j \in \mathbb{N}_n} \sum_{\alpha, \beta, \gamma \in \mathbb{N}_q} \int_0^t z_{\alpha, s}^j H_{\alpha\beta}(s, x_n^j) G_{\beta\gamma}(s, x_n^j) dW_{\gamma, s}^j.$$

Now our assumptions on the diffusion coefficient dictate that the singular values of $G_{\alpha\beta}(s, x_n^j)$ possess (i) a uniform upper bound and (ii) a strictly positive lower bound. This implies that the operator norm of $H(s, x_n^j)$ is uniformly upperbounded by some constant \bar{C} , for all $s \leq T$, all $j \in \mathbb{N}_n$ and all $n \geq 1$. We thus find that there is a constant $c > 0$ such that

$$(6.21) \quad \frac{1}{2n} \left| \sum_{j \in \mathbb{N}_n} \sum_{\alpha, \beta \in \mathbb{N}_q} \int_0^T z_{\beta, s}^j z_{\alpha, s}^j H_{\alpha\beta}(s, x_n^j) ds \right| \leq \frac{c}{2n} \sum_{j \in \mathbb{N}_n} \sum_{\alpha \in \mathbb{N}_q} \int_0^T (z_{\alpha, s}^j)^2 ds.$$

Our assumption on the connectivity in Hypothesis 3.5 implies that

$$(6.22) \quad \frac{c}{2n} \sum_{j \in \mathbb{N}_n} \sum_{\alpha \in \mathbb{N}_q} \int_0^T (z_{\alpha, s}^j)^2 ds \rightarrow 0$$

as $n \rightarrow \infty$, at a uniform rate.

It thus remains to prove that for arbitrary $\varepsilon > 0$,

$$(6.23) \quad \overline{\lim}_{n \rightarrow \infty} n^{-1} \log \mathbb{P}(|X_T| \geq \varepsilon) \leq -\ell.$$

Now X_t is a Martingale, and our assumptions imply that its quadratic variation possesses a uniform upperbound of the form, for some constant $C > 0$ (C is independent of n),

$$(6.24) \quad qv(t) \leq Cn^{-2} \sum_{j \in \mathbb{N}_n} \sum_{\alpha \in \mathbb{N}_q} \int_0^t (z_{\alpha,s}^j)^2 ds.$$

Thus, thanks to Hypothesis 3.5, there must exist a non-random sequence $(\varepsilon_n)_{n \geq 1}$ such that (i) $\lim_{n \rightarrow \infty} \varepsilon_n = 0$ and (ii)

$$(6.25) \quad nqv(T) \leq \varepsilon_n.$$

Using the fact that a continuous martingale can be represented as a time-rescaled Brownian Motion $w(t)$ (see [41]),

$$(6.26) \quad \mathbb{P}(|X_T| \geq \varepsilon) \leq \mathbb{P}\left(\sup_{t \leq n^{-1}\varepsilon_n} |w(t)| \geq \varepsilon\right).$$

Since $\varepsilon_n \rightarrow 0$, standard properties of Brownian Motion [60] dictate that

$$\overline{\lim}_{n \rightarrow \infty} n^{-1} \log \mathbb{P}\left(\sup_{t \leq n^{-1}\varepsilon_n} |w(t)| \geq \varepsilon\right) = -\infty,$$

as required. \square

We are now ready to prove Theorem 6.4.

Proof. We start with the upperbound (6.13). Define the event

$$\mathcal{V}_\delta^n = \{|\Gamma_n(u)| \leq \delta\}.$$

Let $\mathcal{O} \subset Y_T$ be open. Then,

$$\begin{aligned} \underline{\lim}_{n \rightarrow \infty} n^{-1} \log \mathbb{P}(\hat{\mu}_T^n \in \mathcal{O}) &\geq \underline{\lim}_{n \rightarrow \infty} n^{-1} \log \mathbb{P}(\hat{\mu}_T^n \in \mathcal{O}, \mathcal{V}_\delta^n) \\ &\geq -\delta + \underline{\lim}_{n \rightarrow \infty} n^{-1} \log \mathbb{P}(\hat{\mu}_T^n \in \mathcal{O}, \mathcal{V}_\delta^n), \end{aligned}$$

by using (6.16) to change variables. Now

$$\mathbb{P}(\hat{\mu}_T^n \in \mathcal{O}, \mathcal{V}_\delta^n) = \mathbb{P}(\hat{\mu}_T^n \in \mathcal{O}) - \mathbb{P}(\hat{\mu}_T^n \in \mathcal{O}, (\mathcal{V}_\delta^n)^c).$$

Furthermore, it follows from Lemma 6.5 that

$$(6.27) \quad \overline{\lim}_{n \rightarrow \infty} n^{-1} \log \mathbb{P}(\hat{\mu}_T^n \in \mathcal{O}, (\mathcal{V}_\delta^n)^c) = -\infty.$$

We thus find that

$$\underline{\lim}_{n \rightarrow \infty} n^{-1} \log \mathbb{P}(\hat{\mu}_T^n \in \mathcal{O}, \mathcal{V}_\delta^n) = \underline{\lim}_{n \rightarrow \infty} n^{-1} \log \mathbb{P}(\hat{\mu}_T^n \in \mathcal{O}) \geq -\inf_{\mu \in \mathcal{O}} \mathcal{J}_T(\mu),$$

using the LDP lower bound in Lemma 6.3. Taking $\delta \rightarrow 0$, we therefore obtain that

$$\underline{\lim}_{n \rightarrow \infty} n^{-1} \log \mathbb{P}(\hat{\mu}_T^n \in \mathcal{O}) \geq -\inf_{\mu \in \mathcal{O}} \mathcal{J}_T(\mu).$$

Turning to the upperbound, let $\mathcal{A} \subset Y_T$ be closed. Then for any $\delta > 0$,

$$\begin{aligned}\overline{\lim}_{n \rightarrow \infty} n^{-1} \log \mathbb{P}(\hat{\mu}_T^n \in \mathcal{A}) &\leq \max \left\{ \overline{\lim}_{n \rightarrow \infty} n^{-1} \log \mathbb{P}(\hat{\mu}_T^n \in \mathcal{A}, \mathcal{V}_\delta^n), \overline{\lim}_{n \rightarrow \infty} n^{-1} \log \mathbb{P}((\mathcal{V}_\delta^n)^c) \right\} \\ &= \overline{\lim}_{n \rightarrow \infty} n^{-1} \log \mathbb{P}(\hat{\mu}_T^n \in \mathcal{A}, \mathcal{V}_\delta^n),\end{aligned}$$

thanks to Lemma 6.5. Thanks to Girsanov's Theorem (i.e. (6.16)),

$$\overline{\lim}_{n \rightarrow \infty} n^{-1} \log \mathbb{P}(\hat{\mu}_T^n \in \mathcal{A}, \mathcal{V}_\delta^n) \leq \delta + \overline{\lim}_{n \rightarrow \infty} n^{-1} \log \mathbb{P}(\hat{\mu}_T^n \in \mathcal{A}).$$

Using the LDP upperbound of Lemma 6.3,

$$(6.28) \quad \overline{\lim}_{n \rightarrow \infty} n^{-1} \log \mathbb{P}(\hat{\mu}_T^n \in \mathcal{A}) \leq - \inf_{\mu \in \mathcal{A}} \mathcal{J}_T(\mu),$$

and hence after taking $\delta \rightarrow 0^+$ we find that

$$(6.29) \quad \overline{\lim}_{n \rightarrow \infty} n^{-1} \log \mathbb{P}(\hat{\mu}_T^n \in \mathcal{A}) \leq - \inf_{\mu \in \mathcal{A}} \mathcal{J}_T(\mu). \quad \square$$

6.4. Limiting Equations. We finish by proving the almost-sure convergence of Theorem 3.9. We will do this by showing that the rate function \mathcal{J}_T has a unique zero.

Proof. We first notice that \mathcal{J}_T has a unique zero, written as $\nu_* \in X_T$. ν_* can be written as the law of random variables (x, u_0, w) that are such that: (i) the law of (x, u_0) is κ and (ii) the law of $w \in C([0, T], \mathbb{R}^q)$, conditionally on the other variables, is $\mathcal{W}_T(x)$. This fact follows from the definition in (6.3), since $\mathcal{R}(\alpha || \mathcal{W}_T(x))$ is strictly positive, except when $\alpha = \mathcal{W}_T(x)$, in which case it is identically zero [21].

Write $B_\varepsilon(\nu_*) \subset X_T$ to be the ε -ball about ν_* (with respect to the Wasserstein Distance). The Large Deviations Upperbound (6.4) thus implies that

$$(6.30) \quad \overline{\lim}_{n \rightarrow \infty} n^{-1} \log \mathbb{P}(\tilde{\mu}_T^n \notin B_\varepsilon(\nu_*)) < 0.$$

Since Φ_T is continuous, and we have the identity (6.12), we therefore find that

$$(6.31) \quad \overline{\lim}_{n \rightarrow \infty} n^{-1} \log \mathbb{P}(\hat{\mu}_T^n \notin \Phi_T(B_\varepsilon(\nu_*))) = \overline{\lim}_{n \rightarrow \infty} n^{-1} \log P^n(\tilde{\mu}_T^n \notin B_\varepsilon(\nu_*)) < 0.$$

Thus \mathcal{J}_T must have a unique zero at $\Phi_T(\nu_*)$. Thus for any $k \in \mathbb{Z}^+$,

$$(6.32) \quad \overline{\lim}_{n \rightarrow \infty} n^{-1} \log \mathbb{P}(d_{Y_T}(\hat{\mu}_T^n, \Phi_T(\nu_*)) \geq k^{-1}) < 0,$$

thanks to the Large Deviations upperbound of Theorem 6.4. Furthermore, since

$$(6.33) \quad \sum_{n=1}^{\infty} \mathbb{P}(d_{Y_T}(\hat{\mu}_T^n, \Phi_T(\nu_*)) \geq k^{-1}) < \infty.$$

by the Borel-Cantelli Lemma, with unit probability

$$\overline{\lim}_{n \rightarrow \infty} d_{Y_T}(\hat{\mu}_T^n, \Phi_T(\nu_*)) < k^{-1}.$$

Since $k \in \mathbb{Z}^+$ is arbitrary, with unit probability it must be that

$$\lim_{n \rightarrow \infty} d_{Y_T}(\hat{\mu}_T^n, \Phi_T(\nu_*)) = 0.$$

To finish, we characterize $\Phi_T(\nu_*) := \mu$. From the definition of the mapping Φ_T , $\mu \in \mathcal{P}(D \times C([0, T], \mathbb{R}^q))$ is the law of random variables (x, v) , where (x, v_0) is distributed according to κ , and (conditionally on x), for Brownian Motions $\{W_{\alpha,t}\}_{1 \leq \alpha \leq q}$ that are independent of the initial conditions,

$$(6.34) \quad dv_{\alpha,t} = \left(- \sum_{\beta=1}^q L_{\alpha\beta} v_{\beta,t} + I_{\alpha}(t, x) + \sum_{\beta=1}^q \int \mathcal{K}_{\alpha\beta}(x, y) f_{\beta}(\tilde{v}_s) \mu(dy, d\tilde{v}) \right) dt \\ + \sum_{\beta=1}^q G_{\alpha\beta,t}(x) dW_{\beta,t}.$$

Standard theory dictates that (i) there is a unique strong solution to (6.34) and (ii) the solution $v_{\alpha,t}$ is Gaussian (conditionally on x) [41]. The equations governing the evolution of the mean and variance (as outlined in Section 3.5) follow immediately (see for instance [41, Section 5.6]). \square

7. Conclusion. We have formally derived a neural-field equation from a high-dimensional system of neurons on a disordered network. Our aim in this paper has been to strike a balance between biophysical accuracy (insofar as the equations are rigorously proved from a microscopic neural network model) and mathematical tractability (we obtain Gaussian limiting equations, which lead to limiting equations with no spatial derivatives and a very similar structure to the classical Wilson Cowan equations [78]). We were able to determine a range of interesting bifurcations, including local ‘bump’ excitations of neural activity, and spatially structured spiral waves.

There are numerous directions for future research. We wish to more fully explore the dynamics of the limiting equations in Lemma 3.10. After the variance has relaxed to equilibrium, these equations have the form of the classical Wilson-Cowan equations, except with a different firing-rate function. One thus expects that many of the patterns that have already been found in neural field equations [36, 26, 25] can also be found for the equations in Lemma 3.10. A significant advantage of our equations is that one has a more concrete understanding of how exactly they arise out of a particle model.

Another promising avenue is to extend these results to include delays due to synaptic processing / transmission. One expects this to yield fundamentally different limiting equations, since we have $O(n\varphi_n)$ extra synaptic variables.

Finally, for parameterizations involving two or more attractors, we will leverage the Large Deviations result to compute the most likely transition paths between attractors. As we briefly surveyed in the Introduction, it is widely conjectured in the Theoretical Neuroscience community that noise-induced transitions in large ensembles of neurons occur regularly in the brain (in scenarios such as binocular rivalry [59] and UP /DOWN transitions). For even moderately large ensembles of neurons $n > O(100)$ a direct computation of (say) an expected transition time from one attractor to another is completely computationally intractable. Since the Large Deviations rate function gives an asymptotic estimate for the probability of a particular transition pathway, it provides a computationally-tractable means of estimating the likelihood of a transition. Let us note that using the Large Deviations theory to estimate most likely transition pathway will likely still be very computationally demanding, since it requires one to minimize an infinite-dimensional function. However the key difference is that the Large Deviations computational complexity does not diverge with n .

8. Acknowledgements. James MacLaurin would like to acknowledge funding from NSF DMS-2511615.

Appendix A. Proof of Lemma 4.1.

Proof. Fix $x \in D$, set $V_x(t) = V(x, t)$, $G_x = G(x)G^T(x)$, and rewrite the second and fourth equation in (3.8) as the following ODE on $\mathbb{R}^{q \times q}$

$$\frac{d}{dt}V_x = -(LV_x + V_x L^T) + G_x G_x^T, \quad V_x(0) = V_{x,0},$$

whose equilibria satisfy a Sylvester equation. The dynamical system can be transplanted on \mathbb{R}^{q^2} using the vectorisation operator, setting $v_x = \text{vec } V_x$, $g_x = \text{vec}(G_x G_x^T)$, and $M = I_q \otimes L + L^T \otimes I_q$, where I_q is the identity in $\mathbb{R}^{q \times q}$, leading to

$$(A.1) \quad \frac{d}{dt}v_x = -Mv_x + g_x, \quad v_x(0) = v_{x,0}.$$

We note that

$$\sigma(M) = \{\lambda + \rho : \lambda, \rho \in \sigma(L)\}, \quad \max_{\lambda \in \sigma(M)} \operatorname{Re} \lambda < -2\gamma,$$

hence from standard ODE theory it follows that: (i) There exists a unique equilibrium v_x^* to (A.1). (ii) The unique solution to (A.1) is given by

$$v_x(t) = e^{-tM}v_{x,0} + \int_0^t e^{-(t-s)M}g_x ds.$$

(iii) By [35, Definition 3.12–Theorem 3.14] there exist $\beta, \varepsilon > 0$ such that

$$\|v_x(t) - v_x^*\|_{\mathbb{R}^{q^2}} \leq \beta e^{-\varepsilon t} \|v_{x,0} - v_x^*\|_{\mathbb{R}^{q^2}}.$$

The result now follows from recalling that $\|V_x(t)\|_F = \|v_x(t)\|_{\mathbb{R}^{q^2}}$ and noting that, since the mappings $x \mapsto G_x$ and $x \mapsto V_0(x)$ are in $C(D, \mathbb{R}^{q \times q})$, then so is $x \mapsto v_x(t)$ for any $t \in \mathbb{R}_{\geq 0}$. \square

REFERENCES

- [1] Z. P. ADAMS AND J. MACLAURIN, *The isochronal phase of stochastic pde and integral equations: Metastability and other properties*, Journal of Differential Equations, 414 (2025), pp. 773–816.
- [2] Z. AGATHE-NERINE, *Multivariate hawkes processes on inhomogeneous random graphs*, Stochastic Processes and their Applications, 152 (2022), pp. 86–148.
- [3] S.-I. AMARI, *Homogeneous nets of neuron-like elements*, Biological Cybernetics, 17 (1975), pp. 211–220, <https://doi.org/10.1007/BF00339367>.
- [4] D. AVITABILE, *Numerical Computation of Coherent Structures in Spatially-Extended Systems*, May 2020, <https://doi.org/10.5281/zenodo.3821169>, <https://doi.org/10.5281/zenodo.3821169>.
- [5] D. AVITABILE, *Projection Methods for Neural Field Equations*, SIAM Journal on Numerical Analysis, 61 (2023), pp. 562–591, <https://doi.org/10.1137/21M1463768>.
- [6] D. AVITABILE, *Tutorials on Numerical and Analytical Methods for Spatially-Extended Neuronal Networks*, 04 2024, <https://doi.org/10.5281/zenodo.11124322>, <https://github.com/danieleavitabile/numerical-analysis-mathematical-neuroscience>.
- [7] D. AVITABILE, J. L. DAVIS, AND K. WEDGWOOD, *Bump Attractors and Waves in Networks of Leaky Integrate-and-Fire Neurons*, SIAM Review, 65 (2023), pp. 147–182, <https://doi.org/10.1137/20M1367246>.

- [8] D. AVITABILE, M. DESROCHES, R. VELTZ, AND M. WECHSELBERGER, *Local Theory for Spatio-Temporal Canards and Delayed Bifurcations*, SIAM Journal on Mathematical Analysis, 52 (2020), pp. 5703–5747, <https://doi.org/10.1137/19M1306610>.
- [9] D. AVITABILE AND J. MACLAURIN, *Code for the paper 'Neural fields and noise-induced patterns in neurons on large disordered networks'*, 2025, <https://doi.org/10.5281/zenodo.14616641>, <https://doi.org/10.5281/zenodo.14616641>.
- [10] L. BERTINI, G. GIACOMIN, AND C. POQUET, *Synchronization and random long time dynamics for mean-field plane rotators*, Probability Theory and Related Fields, 160 (2014), pp. 593–653.
- [11] T. BIANCALANI, F. JAFARPOUR, AND N. GOLDENFELD, *Giant amplification of noise in fluctuation-induced pattern formation*, Physical review letters, 118 (2017), p. 018101.
- [12] C. BICK AND D. SCLOSA, *Dynamical systems on graph limits and their symmetries*, Journal of Dynamics and Differential Equations, (2024), pp. 1–36.
- [13] P. BILLINGSLEY, *Convergence of probability measures*, John Wiley & Sons, 2013.
- [14] C. BORGES, J. CHAYES, H. COHN, AND Y. ZHAO, *An theory of sparse graph convergence i: Limits, sparse random graph models, and power law distributions*, Transactions of the American Mathematical Society, 372 (2019), pp. 3019–3062.
- [15] J. BRAMBURGER AND M. HOLZER, *Pattern formation in random networks using graphons*, SIAM Journal on Mathematical Analysis, 55 (2023), pp. 2150–2185.
- [16] P. BRAUNSTEINS, F. DEN HOLLANDER, M. MANDJES, ET AL., *A sample-path large deviation principle for dynamic erdős-rényi random graphs*, The Annals of Applied Probability, 33 (2023).
- [17] M. BREAKSPEAR, *Dynamic models of large-scale brain activity*, Nature neuroscience, 20 (2017), pp. 340–352.
- [18] P. C. BRESSLOFF, *Spatiotemporal dynamics of continuum neural fields*, Journal of Physics A: Mathematical and Theoretical, 45 (2011), p. 033001.
- [19] P. C. BRESSLOFF, *Waves in Neural Media*, Lecture Notes on Mathematical Modelling in the Life Sciences, Springer New York, New York, NY, 2014, <https://doi.org/10.1007/978-1-4614-8866-8>.
- [20] P. C. BRESSLOFF AND J. M. NEWBY, *Path integrals and large deviations in stochastic hybrid systems*, Physical Review E, 89 (2014), p. 042701.
- [21] A. BUDHIRAJA AND P. DUPUIS, *Analysis and Approximation of Rare Events*, vol. 94, Springer, 2019, <http://link.springer.com/10.1007/978-1-4939-9579-0>.
- [22] J. A. CARRILLO, P. ROUX, AND S. SOLEM, *Noise-driven bifurcations in a nonlinear fokker-planck system describing stochastic neural fields*, Physica D: Nonlinear Phenomena, 449 (2023), p. 133736.
- [23] J. A. CARRILLO, P. ROUX, AND S. SOLEM, *Well-posedness and stability of a stochastic neural field in the form of a partial differential equation*, arXiv preprint arXiv:2307.08077, (2023).
- [24] J. CHEVALLIER, A. DUARTE, E. LÖCHERBACH, AND G. OST, *Mean field limits for nonlinear spatially extended hawkes processes with exponential memory kernels*, Stochastic Processes and their Applications, 129 (2019), pp. 1–27.
- [25] B. J. COOK, A. D. PETERSON, W. WOLDMAN, AND J. R. TERRY, *Neural field models: A mathematical overview and unifying framework*, Mathematical Neuroscience and Applications, 2 (2022).
- [26] S. COOMBES, P. BEIM GRABEN, R. POTTHAST, AND J. WRIGHT, eds., *Neural Fields*, Springer Berlin Heidelberg, Berlin, Heidelberg, 2014, <https://doi.org/10.1007/978-3-642-54593-1>.
- [27] S. COOMBES AND K. C. A. WEDGWOOD, *Neurodynamics: An Applied Mathematics Perspective*, vol. 75 of Texts in Applied Mathematics, Springer International Publishing, Cham, 2023, <https://doi.org/10.1007/978-3-031-21916-0>.
- [28] F. COPPINI, *Long time dynamics for interacting oscillators on graphs*, The Annals of Applied Probability, 32 (2022), pp. 360–391.
- [29] F. COPPINI, E. LUÇON, AND C. POQUET, *Central limit theorems for global and local empirical measures of diffusions on erdős-rényi graphs*, Electronic Journal of Probability, 28 (2023), pp. 1–63.
- [30] G. DECO, M. L. KRINGELBACH, V. K. JIRSA, AND P. RITTER, *The dynamics of resting fluctuations in the brain: metastability and its dynamical cortical core*, Scientific reports, 7 (2017), p. 3095.
- [31] S. DELATTRE, G. GIACOMIN, AND E. LUÇON, *A note on dynamical models on random graphs and fokker-planck equations*, Journal of Statistical Physics, 165 (2016), pp. 785–798.
- [32] S. DELATTRE, G. GIACOMIN, AND E. LUÇON, *A note on dynamical models on random graphs and fokker-planck equations*, Journal of Statistical Physics, 165 (2016), pp. 785–798, <https://doi.org/10.1007/s10955-016-1652-3>.

- [33] M. G. DELGADINO, R. S. GVALANI, AND G. A. PAVLIOTIS, *On the diffusive-mean field limit for weakly interacting diffusions exhibiting phase transitions*, Archive for Rational Mechanics and Analysis, 241 (2021), pp. 91–148.
- [34] A. DEMBO AND O. ZEITOUNI, *Large deviations techniques and applications*, Springer, 2009.
- [35] K.-J. ENGEL AND R. NAGEL, *One-Parameter Semigroups for Linear Evolution Equations*, no. 194 in Graduate Texts in Mathematics, Springer, New York, 2000.
- [36] G. B. ERMENTROUT, S. E. FOLIAS, AND Z. P. KILPATRICK, *Spatiotemporal Pattern Formation in Neural Fields with Linear Adaptation*, in Neural Fields, S. Coombes, P. beim Graben, R. Potthast, and J. Wright, eds., Springer Berlin Heidelberg, Berlin, Heidelberg, 2014, pp. 119–151, https://doi.org/10.1007/978-3-642-54593-1_4.
- [37] G. B. ERMENTROUT AND D. H. TERMAN, *Mathematical Foundations of Neuroscience*, vol. 35 of Interdisciplinary Applied Mathematics, Springer New York, New York, NY, 2010, <https://doi.org/10.1007/978-0-387-87708-2>.
- [38] E. FORGOSTON AND R. O. MOORE, *A primer on noise-induced transitions in applied dynamical systems*, SIAM Review, 60 (2018), pp. 969–1009.
- [39] C. GRAHAM AND S. MÉLÉARD, *Stochastic particle approximations for generalized boltzmann models and convergence estimates*, The Annals of probability, 25 (1997), pp. 115–132.
- [40] X. HUANG, W. C. TROY, Q. YANG, H. MA, C. R. LAING, S. J. SCHIFF, AND J.-Y. WU, *Spiral Waves in Disinhibited Mammalian Neocortex*, The Journal of Neuroscience, 24 (2004), pp. 9897–9902, <https://doi.org/10.1523/JNEUROSCI.2705-04.2004>.
- [41] I. KARATZAS AND S. E. SHREVE, *Brownian Motion and Stochastic Calculus*, vol. 113 of Graduate Texts in Mathematics, Springer, New York, NY, 1998, <https://doi.org/10.1007/978-1-4612-0949-2>.
- [42] J. P. KEENER AND J. M. NEWBY, *Perturbation analysis of spontaneous action potential initiation by stochastic ion channels*, Physical Review E—Statistical, Nonlinear, and Soft Matter Physics, 84 (2011), p. 011918.
- [43] A. L. KRAUSE, E. A. GAFFNEY, P. K. MAINI, AND V. KLIKA, *Introduction to ‘Recent progress and open frontiers in Turing’s theory of morphogenesis’*, Philosophical Transactions of the Royal Society A: Mathematical, Physical and Engineering Sciences, 379 (2021), p. 20200280, <https://doi.org/10.1098/rsta.2020.0280>.
- [44] A. L. KRAUSE, E. A. GAFFNEY, P. K. MAINI, AND V. KLIKA, *Modern perspectives on near-equilibrium analysis of Turing systems*, Philosophical Transactions of the Royal Society A: Mathematical, Physical and Engineering Sciences, 379 (2021), p. 20200268, <https://doi.org/10.1098/rsta.2020.0268>.
- [45] C. R. LAING, *Spiral Waves in Nonlocal Equations*, SIAM Journal on Applied Dynamical Systems, 4 (2005), pp. 588–606, <https://doi.org/10.1137/040612890>.
- [46] C. R. LAING, W. C. TROY, B. GUTKIN, AND G. B. ERMENTROUT, *Multiple Bumps in a Neuronal Model of Working Memory*, SIAM Journal on Applied Mathematics, 63 (2002), pp. 62–97, <https://doi.org/10.1137/S0036139901389495>.
- [47] J.-F. LE GALL, *Brownian motion, martingales, and stochastic calculus*, Springer, 2016.
- [48] B. LINDNER, J. GARCIA-OJALVO, A. NEIMAN, AND L. SCHIMANSKY-GEIER, *Effects of noise in excitable systems*, Physics reports, 392 (2004), pp. 321–424.
- [49] E. LUÇON, *Quenched asymptotics for interacting diffusions on inhomogeneous random graphs*, Stochastic Processes and their Applications, (2020), pp. 1–52, <http://arxiv.org/abs/1811.09229>.
- [50] E. LUÇON AND C. POQUET, *Emergence of oscillatory behaviors for excitable systems with noise and mean-field interaction: a slow-fast dynamics approach*, Communications in Mathematical Physics, 373 (2020), pp. 907–969.
- [51] E. LUÇON AND C. POQUET, *Periodicity induced by noise and interaction in the kinetic mean-field fitzhugh–nagumo model*, Electronic Journal of Probability, (2021).
- [52] E. LUÇON AND C. POQUET, *Existence, stability and regularity of periodic solutions for nonlinear fokker–planck equations*, Journal of Dynamics and Differential Equations, 36 (2024), pp. 633–671.
- [53] J. MACLAURIN, *Large deviations of a network of interacting particles with sparse random connections*, arXiv preprint arXiv:1607.05471.
- [54] J. MACLAURIN, *Phase reduction of waves, patterns, and oscillations subject to spatially extended noise*, SIAM Journal on Applied Mathematics, 83 (2023), pp. 1215–1244.
- [55] J. N. MACLAURIN AND P. C. BRESSLOFF, *Wandering bumps in a stochastic neural field: A variational approach*, Physica D: Nonlinear Phenomena, 406 (2020), p. 132403.
- [56] P. K. MAINI, T. E. WOOLLEY, R. E. BAKER, E. A. GAFFNEY, AND S. S. LEE, *Turing’s model for biological pattern formation and the robustness problem*, Interface focus, 2 (2012), pp. 487–496.

- [57] A. J. MCKANE, T. BIANCALANI, AND T. ROGERS, *Stochastic pattern formation and spontaneous polarisation: the linear noise approximation and beyond*, Bulletin of mathematical biology, 76 (2014), pp. 895–921.
- [58] H. P. MCKEAN, *Elementary solutions for certain parabolic partial differential equations*, Transactions of the American Mathematical Society, 82 (1956), pp. 519–548.
- [59] R. MORENO-BOTE, J. RINZEL, AND N. RUBIN, *Noise-induced alternations in an attractor network model of perceptual bistability*, Journal of neurophysiology, 98 (2007), pp. 1125–1139.
- [60] P. MÖRTERS AND Y. PERES, *Brownian motion*, vol. 30, Cambridge University Press, 2010.
- [61] J. M. NEWBY, *Spontaneous excitability in the morris–lecar model with ion channel noise*, SIAM Journal on Applied Dynamical Systems, 13 (2014), pp. 1756–1791.
- [62] J. M. NEWBY, P. C. BRESSLOFF, AND J. P. KEENER, *Breakdown of fast-slow analysis in an excitable system with channel noise*, Physical review letters, 111 (2013), p. 128101.
- [63] R. I. OLIVEIRA AND G. H. REIS, *Interacting diffusions on random graphs with diverging average degrees: Hydrodynamics and large deviations*, Journal of Statistical Physics, 176 (2019), pp. 1057–1087.
- [64] H. OTHMER AND L. SCRIVEN, *Instability and dynamic pattern in cellular networks*, Journal of Theoretical Biology, 32 (1971).
- [65] H. OTHMER AND L. SCRIVEN, *Non-linear aspects of dynamic pattern in cellular networks*, Journal of Theoretical Biology, 43 (1974).
- [66] J. RANKIN, D. AVITABILE, J. BALADRON, G. FAYE, AND D. J. B. LLOYD, *Continuation of localised coherent structures in nonlocal neural field equations*, SIAM Journal on Scientific Computing, 36 (2014), pp. B70–B93, <https://doi.org/10.1137/130918721>, <https://arxiv.org/abs/1304.7206>.
- [67] M. SCHEUTZOW, *Noise can create periodic behavior and stabilize nonlinear diffusions*, Stochastic processes and their applications, 20 (1985), pp. 323–331.
- [68] Y. SHU, A. HASENSTAUB, AND D. A. MCCORMICK, *Turning on and off recurrent balanced cortical activity*, Nature, 423 (2003), pp. 288–293.
- [69] A.-S. SZNITMAN, *Topics in propagation of chaos*, Ecole d’été de probabilités de Saint-Flour XIX—1989, 1464 (1991), pp. 165–251.
- [70] H. TANAKA, *Limit theorems for certain diffusion processes with interaction*, in North-Holland Mathematical Library, vol. 32, Elsevier, 1984, pp. 469–488.
- [71] J. TOUBOUL, *Mean-field equations for stochastic firing-rate neural fields with delays: Derivation and noise-induced transitions*, Physica D: Nonlinear Phenomena, 241 (2012), pp. 1223–1244, <https://doi.org/https://doi.org/10.1016/j.physd.2012.03.010>, <https://www.sciencedirect.com/science/article/pii/S0167278912000942>.
- [72] J. TOUBOUL, *Spatially extended networks with singular multi-scale connectivity patterns*, Journal of Statistical Physics, 156 (2014), pp. 546–573.
- [73] J. TOUBOUL, G. HERMANN, AND O. FAUGERAS, *Noise-Induced Behaviors in Neural Mean Field Dynamics*, SIAM Journal on Applied Dynamical Systems, 11 (2012), pp. 49–81, <https://doi.org/10.1137/110832392>.
- [74] A. M. TURING, *The chemical basis of morphogenesis*, Philosophical Transactions of the Royal Society of London. Series B, Biological Sciences, 237 (1952), pp. 37–72, <https://doi.org/10.1098/rstb.1952.0012>.
- [75] C. VAN DEN BROECK, J. PARRONDO, AND R. TORAL, *Noise-induced nonequilibrium phase transition*, Physical review letters, 73 (1994), p. 3395.
- [76] R. VAN DER HOFSTAD, *Random Graphs and Complex Networks Vol II*, Cambridge University Press, 2024.
- [77] X.-J. WANG, *Neurophysiological and computational principles of cortical rhythms in cognition*, Physiological reviews, 90 (2010), pp. 1195–1268.
- [78] H. R. WILSON AND J. D. COWAN, *Excitatory and Inhibitory Interactions in Localized Populations of Model Neurons*, Biophysical Journal, 12 (1972), pp. 1–24, [https://doi.org/10.1016/S0006-3495\(72\)86068-5](https://doi.org/10.1016/S0006-3495(72)86068-5).
- [79] C. ZHOU, J. KURTHS, AND B. HU, *Array-enhanced coherence resonance: nontrivial effects of heterogeneity and spatial independence of noise*, Physical review letters, 87 (2001), p. 098101.